SYLVAIN CHAUVETTE

ORIGINE DES ÉTATS ACTIFS SPONTANÉS DANS LE NÉOCORTEX PENDANT LES OSCILLATIONS DU SOMMEIL

Mémoire présenté
à la Faculté des études supérieures de l'Université Laval
dans le cadre du programme de Maîtrise en Neurobiologie
pour l'obtention du grade de maître ès sciences (M.Sc)

FACULTÉ DE MÉDECINE
UNIVERSITÉ LAVAL
QUÉBEC

2006

Résumé

Le sommeil à ondes lentes est composé d'une alternance entre un état actif et un état silencieux dans le système thalamocortical. Les mécanismes produisant l'état actif et l'état silencieux sont inconnus. Afin d'étudier l'origine des états actifs, nous avons procédé à l'enregistrement intracellulaire simultané de 2 à 4 neurones dans un environnement local (<200µm) et dans un environnement distant (jusqu'à 12mm). Aussi, nous avons procédé à l'enregistrement simultané de potentiels de champ locaux (jusqu'à 16). Ces expériences ont été menées chez le chat anesthésié et chez le chat non-anesthésié. Nous avons trouvé que les cellules à bouffées de potentiels d'action ainsi que les cellules situées profondément ont tendance à être les premières à entrer dans l'état actif. Aussi, nous avons observé une grande variabilité dans les délais d'activation des cellules et ce, qu'elles soient situées près l'une de l'autre ou qu'elles soient distantes. De plus, nous avons observé que le déclenchement de l'état silencieux était beaucoup plus synchrone que le déclenchement de l'état actif.

Abstract

The slow-wave sleep is composed of an alternating period of active and silence state in the thalamocortical system. The mechanisms producing the active and silence state are unknown. In order to investigate the origin of active states, we performed simultaneous intracellular recording of 2 to 4 closely located (<200μm) neurons and in a distant environment (up to 12mm). In addition, we performed simultaneous local field potentials (up to 16) recordings. These experiments were conducted on anesthetized and non-anesthetized cats. We found that Intrinsically-Bursting cells and deeply located cells have tendency to lead in the onset of the active state. We also observed a high, but similar, variability in the activation delay for closely located cells as well as for distantly located cells. In addition, we observed that the onset of silent state is much more synchronous than the onset of active state.

Foreword

The following master thesis is presented in the form of two principal scientific articles. The first article will be submitted soon to *Nature neurosciences* and the second article is in revision in *the journal of neuroscience*. For both articles, I collected the majority of experimental data; I also made the majority of analysis for the first article and had a great participation to the analysis for the second article; I participated in the writing of both articles. A general introduction precedes the presentation of these articles and it describes the structural organization of neocortex, the morphological and electrophysiological types of neurons composing the neocortex, the correlation between electrophysiology and morphology, a brief description of the thalamocortical system, the cortical activity during states of vigilance, and finally, the oscillations composing the slow-wave sleep. A general conclusion linking both articles finalizes this master thesis and the bibliography of both the general introduction and the general conclusion is presented at the end of this master thesis. The reference format of each article is presented according to the rules of the journals.

I would like to express all the gratitude to my master supervisor Dr. Igor Timofeev which gave me the opportunity to work in his great lab since my undergraduate studies and who accepted to be also my supervisor for my Ph. D. Without his critics, discussions, corrections, advices, and support, the present study would not have been possible.

I would like to thanks our collaborators Dr. Maxim Volgushev and Mikhail Mukovski for their fruitful collaboration. I would also like to thanks my present colleagues Josée Seigneur, Dragos Nita, Alex Ferecskó, Krisztina Kovács, Reza Zomorrodi, Julien Daigneault, and Eliane Proulx for their general help; I would also like to thanks former colleagues Sofiane Boucetta, Sylvain Crochet, Youssouf Cissé, and Mario Rosanova for their technical teaching, their previous collaboration, and their general help, and Daniella Rodriguez, Pablo Fuentealba, Michel D'Amours, Walter Rubio Alvarez, and Marie-Michèle Rousseau-Clair for their general help.

I would also like to thank Sylvain Crochet, Sofiane Boucetta, Igor Timofeev, Maxime Volgushev, Mikhail Mukovski, and Maxim Bazhenov for their collaboration in the following studies:

- Boucetta S, Chauvette S, Bazhenov M, Timofeev, I Focal Generation of paroxysmal fast runs during electrographic seizures. Epilepsia: submitted.
- Boucetta S, Crochet S, Chauvette S, Timofeev I, Extracellular Ca 2+ fluctuations during slow oscillation affect AHP and modify firing properties of neocortical neurons. Neurosci.: submitted
- Chauvette S, Volgushev M, Timofeev I Origin of spontaneous actives states in local networks during sleep oscillations. Nat Neurosci.: to be submitted
- Crochet S, Chauvette S, Boucetta S, Timofeev I (2005) Modulation of synaptic transmission in neocortex by network activities. Eur J Neurosci 21:1030-1044.
- Mukovski M, Chauvette S, Timofeev I, Volgushev M (2006) Detection of Active and Silent States in Neocortical Neurons from the Field Potential Signal during Slow-Wave Sleep. Cereb Cortex.
- Chauvette S, Volgushev M, Mukovski M, Timofeev I, Precise long-range synchronization of activity and silence in neocortical neurons. J Neurosci: in revision

Finally, I would like to thanks Pierre Giguère for his technical support and Denis Drolet, who retired this year, for his technical support.

Je dédie ce mémoire à mon père Marcel, à ma sœur Chantal et à ma copine Dominique pour tout le support apporté au cours des années, pour tous leurs encouragements et pour toute la confiance et l'amour qu'ils me témoignent.

Table of contents

List of figures

Chapter II

Chapter III

List of abbreviations

ACSF	Artificial cerebrospinal fluid
AHP	After Hyperpolarizing potential
cAMP	Cyclic Adenosine monophosphate
CSD	Current-source density
EEG	Electroencephalogram
EPSP	Excitatory postsynaptic potential
FRB	Fast-Rhythmic Bursting
FS	Fast Spiking
GABA	Gamma-amino-butyric acid
IB	Intrinsically-Bursting
I_h	Hyperpolarisation-activated cation current
$I_{Na(p)}$	Persistent sodium current
I_t	Low-threshold calcium current
IPSP	Inhibitory postsynaptic potential
LDT	Laterodorsal tegmental nuclei
LFP	Local Field Potential
LTS	Low-threshold spike
PPT	Pedunculopontine nuclei
RS	Regular Spiking
REM	Rapid eye movement
sAHP	Short After Hyperpolarizing potential
SD	Standard deviation
SWS	Slow-wave sleep

Chapter I

1. Introduction Générale

L'activité spontanée est une propriété émergente du réseau cortical dans divers états de vigilance qui se produit même en l'absence de stimulus sensoriel ou de n'importe quelle autre source. L'oscillation lente du sommeil est composée d'une alternance entre des états actifs et silencieux. Très peu d'informations sont connues concernant les développements temporaux et spatiaux de l'onde lente. Est-ce que chaque oscillation lente est un évènement presque synchronisé ou est-ce que l'onde se propage dans le cortex? Le but de cette étude était de décrire comment les états actifs du sommeil à ondes lentes sont initiés, d'où elles originent et comment elles se propagent. Quelques évidences suggèrent que les états actifs ont une origine corticale puisque les oscillations lentes ont été observées chez des animaux athalamiques (Steriade et al., 1993b) et d'autres préparations corticales isolées (Sanchez-Vives and McCormick, 2000; Timofeev et al., 2000b), mais elles étaient absentes dans le thalamus d'animaux dont le cortex avait été enlevé (Timofeev et al., 1996). Dans le but d'élucider le mécanisme pour l'initiation de l'état actif, il faut connaître l'organisation structurelle du néocortex et cette introduction décrit l'organisation laminaire et en colonne du néocortex. Une brève revue des connections néocorticales pourrait être utile pour déterminer le mécanisme de l'oscillation lente puisque cette oscillation est générée dans le néocortex. Une brève revue de la transmission synaptique est aussi présentée. Il est aussi important de connaître les différents types morphologiques et électrophysiologiques de neurones qui composent le néocortex dans le but de déterminer si un certain type de cellule est responsable de la génération de l'oscillation lente. Puisque les cellules peuvent être décrites par des critères morphologiques et par des critères électrophysiologiques, il est important de faire des corrélations entre ces deux types de caractérisation.

Bien que l'onde lente ait une origine corticale, le thalamus et le néocortex sont très interconnectés et donc, l'onde lente est réflètée dans le thalamus dorsal et dans le noyau réticulaire thalamique. Une présentation des neurones composant ces deux structures sera fait.

L'oscillation lente est un des rythmes présents dans le sommeil à ondes lentes. Il y a trois différents états de vigilance : éveil, sommeil à mouvement rapides des yeux et le sommeil à ondes lentes. L'onde lente est présente uniquement pendant le sommeil à ondes lentes. Les différents états de vigilance, les rythmes présents dans chacun des états de vigilance et les mécanismes connus de génération de ces rythmes seront présentés. La dernière section de l'introduction est une description des rythmes qui caractérisent le sommeil à ondes lentes avec l'emphase sur l'oscillation lente, ce qui est le cœur du présent mémoire.

Les mécanismes d'initiation des états actifs demeurent inconnus. Trois hypothèses suggèrent que les bases de l'état actif sont (a) une relâche spontanée de médiateur dans une grande population de neurones qui mène occasionnellement à une somation et aux décharges (Timofeev et al., 2000b), (b) une activité intrinsèque spontanée des neurones à décharges par bouffées de potentiels d'action de la couche 5 du néocortex (Sanchez-Vives and McCormick, 2000) et (c) une synchronisation sélective d'un ensemble neuronal structuré dans l'espace impliquant un petit nombre de cellules (Cossart et al., 2003). Afin de vérifier ces hypothèses, nous avons enregistré l'activité simultanée de potentiel de champs ainsi que l'activité intracellulaire de 2, 3 ou 4 neurones situés près l'un de l'autre (<200 μm) ou loin l'un de l'autre (jusqu'à 12 mm) ou plusieurs potentiels de champs équidistants (jusqu'à 16) avec une Sonde Michigan dans un axe perpendiculaire à la surface du cortex chez des animaux anesthésiés et non anesthésiés. La plupart des neurones enregistrés intracellulairement chez les chats anesthésiés ont été colorés à la neurobiotine.

Nous avons trouvé que dans les neurones séparés d'une dizaine à une centaine de micromètres et pour les neurones séparés par quelques millimètres, n'importe quel neurone du groupe pouvait être le premier à révéler le déclenchement de l'activité avec une tendance pour les neurones à décharges par bouffées de potentiels d'action et pour les neurones situés plus profondément à être les premiers à révéler l'état actif. Le déclenchement de l'état actif pouvait être retardé par un temps aussi long que 50 ms, cependant le taux moyen de délais entre 2 neurones était de 8.0 ± 4.2 ms. Dans nos enregistrements intracellulaires simultanés de 2 à 4 neurones séparés par de longues

distances (approximativement 4-12 mm entre chaque neurone), nous avons observé des résultats similaires, n'importe quel neurone pouvait entrer dans l'état actif en premier et le temps de déclenchement de l'état actif était aussi très variable. La plupart du temps, les périodes actives de l'oscillation lente ont débuté à la bordure des aires 5 et 7 et se sont propagées dans les directions postérieure et antérieure.

1.1 General Introduction

Spontaneous activity is an emergent property of the cortical network in various states of vigilance that occurs even in the absence of sensory stimuli or any other inputs. Slow sleep oscillation is composed of alternations of active and silent states. Little is known about the spatial and temporal development of the slow oscillation. Is each slow oscillation a near-synchronous event or does it spread through the cortex? The goal of this study was to describe how active states of the slow wave sleep are initiated, where do they originate from, and how do they propagate. Some evidences suggest that active state has a cortical origin since the slow oscillation was observed in athalamic animals (Steriade et al., 1993b) and other isolated cortical preparations (Sanchez-Vives and McCormick, 2000; Timofeev et al., 2000b), but is absent in the thalamus of decorticated animals (Timofeev and Steriade, 1996). In order to elucidate the mechanism for initiation of the active state, one has to know the structural organization of the neocortex and this introduction describes the laminar and the columnar organization of the neocortex. A brief overview of neocortical connections could be useful to determine the mechanism of generation of the slow oscillation since it is generated in neocortex. A brief overview of the synaptic transmission is also presented. It is also important to know the different morphological and electrophysiological types of neurons that compose the neocortex in order to determine if a particular type of cell would be responsible for the generation of slow oscillation. Since cells can be defined by morphological and electrophysiological criteria, it is important to try to make correlation between these two characterizations.

Although the slow oscillation has a cortical origin, the dorsal thalamus and the neocortex are highly interconnected, and thus, the slow oscillation is reflected in the thalamus and in the thalamic reticular nucleus. A presentation of the neurons composing these two structures will be made.

Slow oscillation is one the rhythms present during slow wave sleep. There are three different states of vigilance: wakefulness, rapid eye movements sleep and slow wave sleep. Slow oscillation is present only during slow wave sleep. Thus, a brief presentation of the

different states of vigilance, their related rhythms, and the known mechanism of generation of these rhythms is presented. The last section of introduction is a description of rhythms that characterize the slow-wave sleep with emphasis on the slow oscillation, which is the core of the present thesis.

The mechanisms underlying the initiation of active state remain unknown. Three hypotheses suggest that the basis of active states is (a) spontaneous mediator release in a large population of neurons leading to occasional summation and firing (Timofeev et al., 2000b), (b) spontaneous intrinsic activity in layer 5 intrinsically bursting neurons (Sanchez-Vives and McCormick, 2000) and (c) the selective synchronization of spatially structured neuronal ensembles involving a small number of cells (Cossart et al., 2003). To resolve such contradictory conclusions on the origin of active network states we performed simultaneous dual, triple or quadruple intracellular recording of closely located neurons (<200 μm) or distantly located (up to 12 mm) and we also performed multisite equidistant local field potential recordings (up to 16) with a Michigan Probe in a perpendicular axis to the neocortex surface in anesthetized and non-anesthetized cats. Most of the neurons recorded intracellularly in anesthetized cats were stained with neurobiotine.

We found that in neurons separated by tens to hundred micrometers or by few millimeters, any neuron could be the first to reveal the onset of activity with tendency for intrinsically-bursting neurons and deeply located neurons to be the first to reveal active state. The onset of active state could be delayed by as much as 50 ms, but the averaged delay between two neurons was of 8.0 ± 4.2 ms. In our distant recordings (approximately 4-12 mm between each neurons), we observed similar results, any neuron could lead the active state and the onset of active states was also highly variable. Most of the time, the active periods of slow waves started at the border of areas 5 and 7, and propagated to anterior and posterior directions.

1.2 Structural organization of neocortex

The neocortex is superficial part of brain. The thickness of neocortex is 3-4 mm in human and 2 mm in cats.

1.2.1 Laminar organization

The neocortex is formed of six layers with layer one being the most superficial. In humans, the neocortex contains up to 28 x 10^9 neurons and approximately the same number of glial cells (Mountcastle, 1997).

1.2.2 Columnar organization

Neocortex has columnar organization. All columns have similar structure and interconnections (Mountcastle, 1997). In primates, there are about 80 to 100 neurons per minicolumn (Mountcastle, 1997; Buxhoeveden and Casanova, 2002b) and the size vary from 20 to 60 μm (for a review, see (Buxhoeveden and Casanova, 2002a, b)). There are almost no differences in the diameter of minicolumns between species (Mountcastle, 1997). Even if the species are very different, the diameter of macrocolumns is always around 600μm (Mountcastle, 1997; Hustler and Galuske, 2003). The difference between a rat brain and a human brain, in term of minicolumns, is the number of minicolumns, and not the diameter of minicolumns nor the number of containing neurons. Most of the connections run in a vertical way, and columns of similar specificity are connected by long-range horizontal connections (Gilbert and Wiesel, 1989; Hustler and Galuske, 2003).

1.2.3 Neocortical connections

1.2.3.1 The excitatory projections

The main targets of thalamic inputs to the cortex arrive to layer 4, layer 6, and to lower part of layer 3 (DeFelipe and Farinas, 1992; Thomson and Bannister, 2003). This means that the layer 4 cells and every cell that have dendrites in layer 4 could receive inputs from thalamus, but generally synapses from thalamus projections are located on spines of basal dendrites very close to the soma of pyramidal cells (Somogyi et al., 1998) and on large basket cells and neurogliaform cells (Mountcastle, 1998). Then, the axons of

layer 4 spiny excitatory cells (pyramidal and spiny stellate cells) send information to layer 3 cells (Lund, 1973; Valverde, 1976; Parnavelas et al., 1977; Feldman and Peters, 1978; Gilbert and Wiesel, 1979; Gilbert, 1983; Burkhalter, 1989; Anderson et al., 1994; Watts and Thomson, 2005). There are many excitatory connections originating from layer 3 cells, some of them project in the same layer (layer3-layer3) (Rockland and Lund, 1982; Kisvarday et al., 1986; McGuire et al., 1991), whereas other excitatory connections originating from layer 3 project to layer 2, and also to layer 5 (Lorente de No, 1922; Spatz et al., 1970; Gilbert and Wiesel, 1983; Kisvarday et al., 1986; Burkhalter, 1989; Lund et al., 1993; Yoshioka et al., 1994; Kritzer and Goldman-Rakic, 1995; Fujita and Fujita, 1996). Layer 3 is also the target and the source of callosal projection innervating symmetrical point in contralateral cortex (Mountcastle, 1998; Cisse et al., 2003; Thomson and Bannister, 2003). Even if the intracortical axons pass through layer 4, they do not or almost do not arborize in this layer. The layer 5 cells interact mainly with other layer 5 cells, but can also project to all other layers (Burkhalter, 1989; Keller, 1993; Yoshioka et al., 1994; Fujita and Fujita, 1996). Presynaptic layer 5 pyramidal cells that are hundreds of microns from their pyramidal target innervate more distal regions (Deuchars et al., 1994), while those that are close neighbours contact basal and/or apical oblique dendritic branches (Markram and Tsodyks, 1996; Markram et al., 1997). There are excitatory inputs from layer 5 to layer 3 interneurons (Thomson et al., 1996; Callaway, 2002). The layer 6 cells don’t receive or receive only a weak, but focused, information from superficial layer, but their axons arborize in layer 4 and 5 (Gilbert and Wiesel, 1979; Zhang and Deschenes, 1997; Thomson and Bannister, 2003; Watts and Thomson, 2005) and also project to the thalamus (Somogyi et al., 1998). Layer 6 pyramidal axons often arborize densely in layer 4 (Gilbert and Wiesel, 1979) and in layer 5, and also the pyramidal axons of layer 6 simple cells project to layer 4, while complex cells project to layers 2 and 3 (Hirsch et al., 1998). Layer 2 and 3 receive the majority of corticocortical projections (Gilbert and Wiesel, 1989).

1.2.3.2 The inhibitory projections

Layer 3 cells receive inhibitory projections mainly from layer 4 (Lund, 1987, 1988; Thomson et al., 2002; Thomson and Bannister, 2003; Watts and Thomson, 2005). Inhibitory inputs to layer 4 are from layer 4, 5, and 6 (Lund, 1988; Thomson et al., 1996),

but also from some layer 3 interneurons (Somogyi and Cowey, 1981; Tamas et al., 1998). In primates, the interneurons in layer 5A innervate all the layers that receive thalamic inputs: layer 4A, 4C, 6, 3 as well as layer 1 and 2 (Lund, 1988). Inhibitory projections to layer 5 and 6 are from layer 3 and 4, but they are mainly weak or focused (Lund, 1988; Thomson and Bannister, 2003; Watts and Thomson, 2005). Most interneurons innervate mainly neurons in their layer of origin.

1.2.4 Synaptic transmission

Both electric and chemical synapses are present in neocortex. So far, electrical synapses in neocortex have been found between inhibitory neurons (Galarreta and Hestrin, 1999; Gibson et al., 1999; Galarreta and Hestrin, 2001). Possibly, axons of some pyramidal cell are also electrotonically coupled (Schmitz et al., 2001). There are two kinds of chemical synapses: symmetric and asymmetric. The symmetric synapses are inhibitory and the asymmetric synapses are excitatory (Colonnier, 1981). Some characteristics of asymmetric synapses are the high density in the cytoplasmic face of the postsynaptic cell and their vesicles that are spherical (Peters et al., 1991; DeFelipe and Farinas, 1992). However, symmetric synapses are characterized by pleomorphic vesicles and by thin postsynaptic density (Peters et al., 1991). The main target of pyramidal cells are others pyramidal cells and the synapses are almost exclusively located on spines, but sometimes on dendritic shaft of other pyramidal neurons, and pyramidal cells also innervate GABAergic cells (McGuire et al., 1984; Kisvarday et al., 1986; Gabbott et al., 1987; McGuire et al., 1991; Somogyi et al., 1998). A pyramidal cell may have up to 8 synaptic terminals on one postsynaptic cell (Markram et al., 1997; Somogyi et al., 1998; Krimer and Goldman-Rakic, 2001). From 10 to 20 inputs arriving from pyramidal cells are necessary to bring a GABAergic cell to threshold (Thomson and Deuchars, 1997; Somogyi et al., 1998). The amplitude of excitatory postsynaptic potential (EPSP) *in vitro* is variable. Generally, it ranges from 0.1 to 2 mV, (but sometimes up to 9 mV) with a total mean of about 1 mV (Thomson et al., 1995; Stratford et al., 1996; Buhl et al., 1997; Markram et al., 1997; Krimer and Goldman-Rakic, 2001). In intact cortex in vivo, the single-axon responses range from failures to 1.5 mV, with mean amplitude of 0.71 ± 0.31 mV (Crochet et al., 2005).

Gamma-amino-butyric acid (GABA) is the major inhibitory neurotransmitter and its effects include a shunting of excitatory currents in dendrites, and hyperpolarizing inhibition (Borg-Graham et al., 1998; Somogyi et al., 1998). In hyperpolarizing inhibition, negative and positive currents sum linearly to produce a net change in membrane potential, in contrast, shunting inhibition acts nonlinearly by causing an increase in membrane conductance; this divides the amplitude of the excitatory response (Borg-Graham et al., 1998). Pyramidal cells receive many inputs; it has been estimated that a cortical neuron may receive up to 60 000 synapses on their soma, their dendritic shaft, their spines, and on their axon initial segment (Cragg, 1967; Peters, 1987). Some studies showed that synapses on the cell body or proximal dendrites are more efficient than synapses that are farther from the soma (DeFelipe and Farinas, 1992; Williams and Stuart, 2002). However, recent studies have shown that it is not a general rule, and that for pyramidal cells in CA1 hippocampus, the somatic amplitude EPSP is independent of synapse location (Magee and Cook, 2000; Williams and Stuart, 2003). Some GABAergic cells are specialized to innervate a specific portion of the cell (Marin-Padilla, 1969, 1974; Marin-Padilla and Stibitz, 1974; Szentagothai and Arbib, 1974; Jones, 1975; Szentagothai, 1975, 1978; Fairen and Valverde, 1980; Hollander and Vanegas, 1981; Peters and Regidor, 1981; Somogyi and Cowey, 1981; Somogyi et al., 1982). Synapses on the cell body have been found to be exclusively inhibitory and of intrinsic cortical origin (symmetric synapses only) (Peters et al., 1991). Basket cells are the major source of synapses on the soma of other cells, but large Basket cells are also known to form synapses on the apical and basal dendrites of pyramidal cells (Somogyi et al., 1983; Somogyi et al., 1998; Squire, 2003). The vast majority of synapses are located on dendritic surface (spines and dendritic shafts), namely 90-95 % of the receptive surface of neurons (Sholl, 1955). Synapses on the dendritic shaft are mainly of symmetric type while those on spines are almost exclusively of asymmetric type (Hersch and White, 1981; White and Hersch, 1981; Hersch and White, 1982; White and Hersch, 1982; Porter and White, 1986). The main source of synapses on spines are other neighboring pyramidal cells (Gilbert and Wiesel, 1979, 1983; Martin and Whitteridge, 1984; DeFelipe et al., 1986; Schwark and Jones, 1989; Ojima et al., 1991), and also the inputs formed by spiny stellate cells of layer IV (LeVay, 1973; Somogyi, 1978;

Mates and Lund, 1983; Saint Marie and Peters, 1985), by some sparsely spiny cells that are called bipolar cells (Peters and Kimerer, 1981; Fairen et al., 1984; Peters and Harriman, 1988), by thalamocortical afferent fibers (Garey and Powell, 1971; Peters and Feldman, 1976), and by corticocortical afferent fibers (Jones and Powell, 1970; Lund and Lund, 1970; Sloper, 1973; Fisken et al., 1975; Sloper and Powell, 1979; Cipolloni and Peters, 1983; Ichikawa et al., 1985; Porter and White, 1986; Porter and Sakamoto, 1988; Voigt et al., 1988; Lowenstein and Somogyi, 1991). However, only one type of sparsely spiny neurons, the bipolar cells, are known to make symmetric synapses on spines (Peters and Kimerer, 1981; Fairen et al., 1984; Peters and Harriman, 1988), and they also synapse on shafts of both pyramidal and nonpyramidal cells (Peters and Kimerer, 1981; Peters and Harriman, 1988). The major source of symmetric synapses on dendritic spines of pyramidal neurons comes from double bouquet cells (DeFelipe and Farinas, 1992). As it was mentioned before, the thalamocortical afferent fibers are excitatory, so they build asymmetric synapses on spines and corticocortical afferent fibers also form asymmetric synapses with spines (White, 1989).

1.3 Morphological types of neurons composing the neocortex

There are many different types of neurons in the cortex, but they are generally classified as pyramidal neurons or nonpyramidal neurons. Among nonpyramidal neurons, there are spiny stellate cells, arcade cells, double bouquet cells, small basket cells, chandelier cells, peptides Y cells, neurogliaform cells, and large basket cells. Pyramidal cells and spiny stellate cells are excitatory cells and both are spiny. All other cortical cells are inhibitory. Some authors prefer to classify the neurons in two classes: spiny neurons and aspiny nonpyramidal neurons.

1.3.1 Pyramidal neurons

Pyramidal cells are long-axon cells that represent up to 80% of all neurons of neocortex in mammalian (DeFelipe and Farinas, 1992; Steriade, 2001a) and they receive 5000 to 60000 synapses (Cragg, 1967; DeFelipe and Farinas, 1992; Mountcastle, 1998; Somogyi et al., 1998). They are represented in all cortical layers except layer 1. Pyramidal cells use glutamate (and/or aspartate) as their excitatory neurotransmitter agent. The main targets of pyramidal neurons are other pyramidal cells and also some extracortical structures (Mountcastle, 1998). In layer 3, ninety-five percent of their targets are other pyramidal cells (Mountcastle, 1998; Squire, 2003). Although all the pyramidal neurons have the same kind of morphology, they differ in spine density, in shape, in size, in dendritic branching, in their pattern of axonal collaterals, and in their projection site (DeFelipe and Farinas, 1992). Some general characteristics of typical pyramidal cells are the shape of the soma, which is pyramidal, or ovoid, the axon comes from the base of the soma on the opposite side of the apical dendrites, all dendrites are spiny and generally, their apical dendrite reaches layer 1 (DeFelipe and Farinas, 1992).

1.3.2 Non-pyramidal neurons

Spiny nonpyramidal cells (spiny stellate cells) are the major target of excitatory thalamocortical fibers (Mountcastle, 1998). These are also excitatory cells and they are mainly confined in layer 4 (Fairen et al., 1984). Spiny stellate cells are also called excitatory interneuron due to their small and multipolar form and because of their local dendrites and axon arborization (Squire, 2003). Their axon collaterals arborize into layer 2

and 3 and 90% of their dendrites are confined to a distance of 60 μm from the soma (Bannister et al., 2002). As for the pyramidal cells, the axon of spiny stellate cells emerges from the white matter side (Bannister et al., 2002) and they use glutamate or aspartate as their neurotransmitter (Squire, 2003). Their targets are spines of pyramidal cells, spines of other spiny stellate cells, and also dendrites of aspiny nonpyramidal inhibitory cells (Mountcastle, 1998).

Aspiny nonpyramidal cells (or sparsely spiny cells) are present in all cortical layers, they have short-axons and many contain GABA, thus suggesting an inhibitory function (Markram et al., 2004). GABAergic cells are a heterogeneous group of neurons that receive on average 4000 to 6000 synapses (Somogyi et al., 1998) and are classified on the basis of their patterns of axonal arborization (Fairen et al., 1984). The dendritic morphology of interneurons is highly variable and cannot reliably define the type of interneuron (Markram et al., 2004). However, the axonal arborization can reveal the anatomical identity of an interneuron because interneurons seem to be particularly specialized to target different domains of neurons, different layers of a column, and different columns (Markram et al., 2004). Interestingly, an axon of a given GABAergic cell can form distinct types of synapses on pyramidal cells, and it was shown that an interaction between the presynaptic and the postsynaptic neurons is involved in formation of the type of synapse (Gupta et al., 2000).

There are two types of inhibitory cells that appear to be less selective than others. First, Martinotti cells, which innervate cells from where they are located up to layer 1 cells, and on the other hand, Double Bouquet cells innervate cells from their origin to layer 5 or 6 cells (Thomson and Bannister, 2003). The Martinotti cells are multipolar and sparsely spiny cells that are located in layer 2 to 6 of the cortex and their axons may synapse in layer 2, 3 or 5, but their main targets are layer 1 cells where their axons run horizontally for more than 500 μm (Wahle, 1993; Markram et al., 2004). The Martinotti cells inhibit mainly the tuft dendrites of pyramidal neurons (Markram et al., 2004), but can also innervate the proximal dendrites, perisomatic dendrites, and soma (Wang et al., 2004). The Double Bouquet cells usually have a bitufted dendritic morphology (Markram et al., 2004) and their special feature is a tight fascicular axonal cylinder that resembles a “horse tail”

(Somogyi and Cowey, 1981; White, 1989; DeFelipe et al., 1990). The Double Bouquet cells mainly target dendrites (shafts and spines) of pyramidal cells, and they are located in layer 2 to layer 5, but seems to be preferentially located in the supragranular layers (Markram et al., 2004). The double bouquet cells are small (diameter of 10-18 μm) and they form synapses on dendritic shafts and little branches of others inhibitory neurons and they also build synapses on spines or small dendritic branches of pyramidal cells (Somogyi and Cowey, 1981; del Rio and DeFelipe, 1995). Their regional, laminar, and synaptic organization suggest that they play a crucial role in the regulation of pyramidal cells output that furnish corticocortical projections (Squire, 2003).

The basket cells represent about 50% of all inhibitory interneurons (Markram et al., 2004) and they are specialized in targeting the soma and proximal dendrites of pyramidal interneurons (Marin-Padilla, 1969; White, 1989; Gilbert, 1993; Wang et al., 2002). The term “basket cell” comes from the basket-like appearance around pyramidal cell soma that result from convergent innervations by many basket cells (Markram et al., 2004). On the basis of differences in their axonal and dendritic morphologies, basket cells can be divided into three main subclasses: large basket cells, small basket cells, and nest basket cells (Markram et al., 2004). The large basket cells are the largest nonpyramidal cells of the neocortex with a soma diameter of 20-33 μm (Mountcastle, 1998), and they innervate perisomatic region of other cells (DeFelipe and Farinas, 1992; Somogyi et al., 1998; Gupta et al., 2000; Squire, 2003). A basket cell can innervate several pyramidal cells and one pyramidal cell can be innervated by numerous basket cells (Squire, 2003). This type of cells, which is mainly located in layer 3 and 5, and also in layer 4 (Gupta et al., 2000), is aspiny, has mainly a multipolar morphology with dendrites extending in all directions for several micrometers, and their axons often bifurcate quickly and travel distance up to 2 mm (Squire, 2003). Large basket cells, usually multipolar, might also have a somato-dendritic morphology that is bitufted, pyramidal or bipolar and they are the primary source of lateral inhibition across columns within the layer that contains their soma (Markram et al., 2004). Small basket cells have the same shape and the same target as large basket cells, but they are only 12 μm in diameter (Fairen et al., 1984). Small basket cells can also be distinguished from large basket cells by their frequently branching and curvy axons

(Markram et al., 2004). The nest basket cells are, as other type of basket cell, soma-targeting (Gupta et al., 2000; Wang et al., 2002) and the "nest" arises because of their birds'-nest-like appearance (Markram et al., 2004). They seem to be an hybrid of large basket cells and small basket cells, but have a local axonal cluster more like small basket cells, and less frequent branching, and longer axonal collaterals with a lower density of boutons, more like large basket cells (Markram et al., 2004).

The axo-axonic cells synapse exclusively in an uniform and specific way, on axons initial segment of pyramidal cells (Somogyi, 1977; Somogyi et al., 1998). They are also called chandelier cells, and they are small neurons with a somatic diameter of 10-15 μm that are localized in layer 2 and 3 (Somogyi, 1977), but could also be found in layer 4, 5, and 6 (Markram et al., 2004). Chandelier cells can be multipolar or bitufted and their local axonal cluster are formed by high-frequency branching at shallow angles, often ramifying around, above or below their soma with a high bouton density (Markram et al., 2004). The characteristic terminal portions of the axon form short vertical rows of boutons, resembling a chandelier (Somogyi, 1977; Somogyi et al., 1982). Each pyramidal cell receives 1 to 3 synapses from chandelier cells, but one chandelier cell inhibits from 100 to 400 pyramidal cells (Marin-Padilla, 1987). It is thought that these cells are able to completely shut down the firing of a pyramidal cell (Squire, 2003).

The peptide Y cells, also called bipolar or bitufted cells, are present in all cortical layers except in layer 4 and even if their targets have not been clearly defined, it is known that their dendrites and their axons arborize vertically in both directions to reach all layers of the cortex (Kuljis and Rakic, 1989).

Neurogliaform cells have been identified as the smallest inhibitory interneurons of the cortex with a diameter of 10 to 12 μm and are located in all layers of the cortex, but are more concentrated in layer 3 and 4 and their targets are thought to be spiny nonpyramidal cells (Jones, 1975). They also have many fine and radiating dendrites that are short, aspiny, finely beaded, and rarely branched (White, 1989). Shortly after its origin, the axon breaks

up into a dense, intertwined arborization of ultra-thin axons with as many as ten orders of branching (Markram et al., 2004).

Layer 1 neurons are virtually all inhibitory and they fall into two categories (Hestrin and Armstrong, 1996). The first comprises Cajal Retzius cells, which are large neurons with horizontal processes, and are multipolar cells with various soma shapes (Markram et al., 2004). Their axons, which are confined to layer 1, can be extensive and typically have a horizontal trajectory, and are believed to target the terminal tufts of pyramidal cells (Markram et al., 2004). The second category is a heterogeneous group of small, multipolar interneurons with varying axonal arborization (Markram et al., 2004).

1.4 Electrophysiological types of neurons composing the neocortex

There are billions of neurons composing the neocortex, and they can be classified in at least 4 electrophysiological groups: Regular-Spiking (RS), Intrinsically-Bursting (IB), Fast-Spiking (FS), and Fast-Rhythmic-Bursting (FRB) (Connors and Gutnick, 1990; Gray and McCormick, 1996; Steriade et al., 1998; Steriade et al., 2001). All these electrophysiological types of neurons can be observed in vitro (FRB can be seen only with artificial cerebrospinal fluid that contains physiological levels of extracellular calcium (Brumberg et al., 2000)) as well as in vivo under anesthesia, or in vivo without anesthesia in any state of vigilance (Steriade et al., 2001). In addition, they can all be observed in all cortical layers (Steriade et al., 1998; Timofeev et al., 2000a; Cardin et al., 2005). RS cells are the most common type of cells recorded in neocortex (Connors and Gutnick, 1990). These cells are characterized by spike frequency adaptation in response to depolarizing current pulses and by the absence of burst response (McCormick et al., 1985). IB cells are characterized by the presence of an initial burst that can be followed either by other bursts or by single spikes (McCormick et al., 1985; Connors and Gutnick, 1990; Nunez et al., 1993). Within a burst, spikes tend to decrease in amplitude and bursts occur at 5-15 Hz (Connors and Gutnick, 1990). The intraburst frequency of FRB cells is between 300 and 600 Hz, and the interburst frequency ranges from 20 to 50 Hz, but is mainly between 30 and 40 Hz (Gray and McCormick, 1996; Steriade et al., 1998; Cardin et al., 2005). The FRB cells differ from IB cells by their regular interspike intervals within a burst while the IB cells generally display a longer first interspike interval (Steriade et al., 1998). In addition, the spikes of FRB cells show a much larger short afterhyperpolarization (sAHP) similar to spikes of FS, while spikes of IB and RS show only a slight sAHP (Steriade et al., 1998). The spikes of FS and FRB cells are thin while spikes of RS and IB are broader (Connors and Gutnick, 1990; Gray and McCormick, 1996; Steriade et al., 1998; Steriade et al., 2001). The FS cells are characterized by a linear current-frequency response to depolarizing current pulses with tonic firing reaching up to 800 Hz, and they don’t show spike frequency adaptation (Connors and Gutnick, 1990; Gray and McCormick, 1996).

1.5 Correlation between electrophysiology and morphology

Many authors have tried to correlate electrophysiology with neuronal morphology (McCormick et al., 1985; Chagnac-Amitai et al., 1990; Connors and Gutnick, 1990; Gray and McCormick, 1996; Timofeev et al., 2000a; Steriade, 2004a). RS cells were thought to be either pyramidal cells or spiny stellate cells while FS were thought to be aspiny non-pyramidal neurons, thus interneuron (Connors and Gutnick, 1990; Gray and McCormick, 1996). There was also a study that showed that in layer 5, IB cells are large pyramidal cells (Chagnac-Amitai et al., 1990). FRB, also called chattering cells, were thought to be layer II/III pyramidal cells (Gray and McCormick, 1996) and more recently were associated with pyramidal cell of any layer (Steriade et al., 1998) or basket cell (Steriade et al., 1998; Steriade, 2004a). Recent studies showed that electrophysiological properties of neurons can be modulated by a change in the network activity (Timofeev et al., 2000b) or by changing the extracellular calcium concentration (Brumberg et al., 2000; Boucetta et al., Submitted 2005). The proportion of IB cells observed in cortical slab preparation was increased with 39% of cells recorded being IB, while 15 to 20% are usually observed in intact cortex (Timofeev et al., 2000b). The presence of norepinephrine and acetylcholine also transforms the burst firing mode of a cell into a tonic firing mode (Wang and McCormick, 1993). Thus cells are able to change their firing pattern. In addition, by injecting slight sustained depolarization in the cells, the neurons converted the burst firing into a RS pattern (Timofeev et al., 2000b; Steriade, 2004a). It is also important to note that these depolarizations can occur naturally with transition from slow-wave sleep to wakefulness or to REM sleep, and thus, the change in state of vigilance can change the firing pattern (Steriade, 2001b; Steriade et al., 2001; Steriade, 2004a). This could be an explanation for the increased proportion of IB cells in cortical slabs (Timofeev et al., 2000b) or in slices (40-60%) (Nishimura et al., 2001) in which the cells are more hyperpolarized, and it could also explain the lower percentage (<5%) of IB cells during wakefulness, a state in which the neurons are more depolarized (Steriade et al., 2001). The change in extracellular calcium concentration to a physiological range (1.0 to 1.2 mM) in artificial cerebrospinal fluid (ACSF) allowed to record cells with FRB pattern (Brumberg et al., 2000) while with traditional ACSF, no FRB cells were reported in vitro. Also, in vivo, with microdialysis

technique, a diminution in the extracellular calcium concentration to approximately 0.8 mM transformed RS cells into IB cells (Boucetta et al., Submitted 2005). Transitions from RS to FRB to FS were also described (Steriade et al., 1998) and these transitions were ascribed to the persistent sodium current ($I_{Na(p)}$) and to a reduction in fast voltage- and calcium-dependant potassium conductances (Traub et al., 2003). Up to now, all FS cells recorded and stained were found to be interneurons, but for the 3 other types, no association between morphology and electrophysiology can be made since the firing pattern is modulated by different factors including the extracellular potassium concentration, the membrane potential, the network activity/state, the presence of neuromodulators, and the extracellular calcium concentration.

1.6 Thalamocortical system

The thalamocortical network is organized in a loop. The main gateway of thalamocortical system is dorsal thalamus, which receives specific inputs from ascending sensory pathways and from the brainstem modulatory systems (Steriade et al., 1997). These thalamocortical neurons send their glutamatergic axons to the cerebral cortex and to the reticular thalamic nucleus (Steriade et al., 1997). The thalamocortical neurons project mainly in the layer IV of neocortex but also few axons of thalamocortical neurons ascending from associative and nonspecific nuclei of dorsal thalamus project to layer I and VI (Steriade et al., 1997). The reticular nucleus receives glutamatergic (excitatory) inputs from collaterals of thalamocortical cells and corticothalamic fibers, all of which pass through the reticular nucleus (Jones, 1985). The excitatory influence of corticothalamic projections is much stronger for reticular nucleus neurons, which are all GABAergic, than for thalamocortical neurons (Golshani et al., 2001). The main axons of reticular cells terminate in the thalamus and a characteristic of the reticular nucleus is the presence of electrical coupling (Landisman et al., 2002; Fuentealba et al., 2004c).

1.6.1 Thalamocortical neurons

The thalamocortical neurons possess many intrinsic currents that enable them to mediate some oscillatory activities. When depolarized, thalamocortical neurons fire in a tonic mode. When hyperpolarized by a current pulse or IPSPs to the level of activation of hyperpolarisation-activated cation current (I_h), the cells respond with a depolarizing sag. During the hyperpolarisation, the low-threshold calcium current (I_t) is deinactivated and at the offset of the current pulse, the I_t is activated and the cell produces a low-threshold spike (LTS) that can lead to a burst of action potentials. This indicates that thalamocortical neurons can fire when they are hyperpolarized and when they are depolarized. Thus, the thalamocortical cells may respond with tonic firing to excitatory inputs, as sensory inputs, while they respond with bursting firing when hyperpolarized (Rosanova and Timofeev, 2005).

1.6.2 Reticular thalamic neurons

Similar to thalamocortical neurons, the reticular neurons can discharge in a burst mode or in a tonic mode (Mukhametov et al., 1970; Steriade and Wyzinski, 1972; Steriade et al., 1986). The firing mode depends on the membrane potential level (Contreras et al., 1992; Bal and McCormick, 1993; Gentet and Ulrich, 2003). At depolarized membrane potential (>-65 mV), intracellular injection of positive current pulse induces tonic firing, while at more hyperpolarized membrane potential (<-65mV), the same intracellular injection of current produces high-frequency bursts (300-500 Hz) of action potentials (Bal and McCormick, 1993; Contreras et al., 1993).

1.7 Cortical activity during states of vigilance

There are three different states of vigilance: wakefulness, slow-wave sleep (SWS), and rapid eye movement (REM) sleep.

1.7.1 Wakefulness

Wakefulness is associated with an activation of brainstem pedunculopontine and laterodorsal tegmental (PPT/LDT) cholinergic nuclei, which blocks low-frequency rhythmic activities (<15Hz) that characterize slow-wave sleep (Steriade, 2000, 2004b). Frequencies such as alpha, mu, theta, beta, and gamma characterize wake state. The alpha rhythm (8 to 13 Hz) is better seen with eyes closed under conditions of physical relaxation and relative mental inactivity; the alpha rhythm disappear with alertness and with sleep (Niedermeyer, 1993a). The amplitude of alpha waves tends to wax and wane and these rhythms are present over occipital, parietal, and posterior temporal regions (in humans) (Niedermeyer, 1993a). The mu rhythms are very similar in shape and in frequency to alpha rhythm, but they are present in somatosensory and motor areas, and they present sharp negative and rounded positive wavelets (Niedermeyer, 1993a). Mu rhythms are blocked by movements and are thought to be related to the conceptual design of the movement to be executed (Niedermeyer, 1993a). Theta frequencies are also present and range from 4 to 7.5 Hz (Niedermeyer, 1993a). The waking state is also characterized by the predominance of beta (15-30 Hz) and gamma (30-60 Hz) frequencies (Bressler, 1990; Freeman, 1991). Gamma is associated with attentiveness (Rougeul-Buser et al., 1975; Bouyer et al., 1981), focused arousal (Sheer, 1989), sensory perception (Gray et al., 1989), and movement (Murthy and Fetz, 1992; Pfurtscheller and Neuper, 1992). Waking state is associated with an activated pattern of EEG, muscle tone, and depolarization and tonic firing of the majority of cortical neurons (Steriade et al., 2001; Timofeev et al., 2001a).

1.7.2 Rapid Eye Movement sleep

The REM sleep was first described in 1937, and was called B state, which consisted in a state of sleep with no alpha rhythm, only low voltage changes in potential, some eyes

rolling, and was associated with dreams (Loomis et al., 1937). The appellation “rapid eye movement period of sleep” was given by Aserinsky and Kleitman, and they remarked that no delta waves could be recorded during rapid eye movement periods, that movements were binocularly synchronous, and that dream recalls were associated with a previous presence of rapid eye movement period (Aserinsky and Kleitman, 1955). It was also suggested that rapid eye movements are involved in visual imagery accompanying dreaming (Aserinsky and Kleitman, 1955). Now, it is well known that REM sleep is associated with an activated pattern of EEG, an absence of muscle tone, the presence of ocular saccades, tonic firing of thalamocortical (Hirsch et al., 1983), and depolarization of cortical neurons (Steriade et al., 2001; Timofeev et al., 2001a).

1.7.3 Slow-Wave sleep

The occurrence of slow rhythms during sleep was first described in 1937 (Blake and Gerard, 1937). Up to now, slow-wave sleep has been divided in four stages. The first one is called drowsiness, in which one can observe a transition from alpha to vertex waves (Niedermeyer, 1993b). The second stage is light sleep during which spindles, vertex waves, and K complexes can be observed (Niedermeyer, 1993b). Deep sleep is the third stage of SWS and is characterized by much slower waves, K complexes, and some spindles (Niedermeyer, 1993b). The fourth stage of sleep is very deep sleep that is again characterized by the presence of much slower waves and K complexes (Niedermeyer, 1993b). The K complex is an EEG pattern that reflects a sequence of depolarizing and hyperpolarizing membrane potentials in cortical neurons (Amzica and Steriade, 2002).

1.8 Oscillations in slow-wave sleep

As for other states of vigilance, slow-wave sleep has different rhythm composing the EEG.

1.8.1 Slow oscillation

The slow oscillation can be observed in natural sleep as well as in anaesthetized animals with urethane, mixture of ketamine and nitrous oxide, and mixture of ketamine and xylazine (Steriade et al., 1993a). It consist in an alternation between an active state and a silent state that is more hyperpolarized by 5 to 25 mV (Steriade et al., 1993a; Contreras and Steriade, 1995; Timofeev et al., 2000b; Steriade et al., 2001; Timofeev et al., 2001a; Mukovski et al., Submitted 2005)). It is now known that the silent state is not due to an active inhibition since (1) FS cell are also hyperpolarized during silent states and they do not fire more at the end of the cycle (2) all neurons that were recorded with potassium chloride to reverse the chloride current (activated via gamma-aminobutyric acid (GABA) receptor) revealed hyperpolarized phase, and (3) all neurons that were recorded with cesium acetate, which blocks most of potassium current, revealed an absence of the hyperpolarized phase during the silent phase of network activity (Timofeev et al., 2001a). Other studies showed that some sleep frequencies were affected by the mutation of a gene responsible for an ion channel that control the membrane repolarization, thus it suggests that potassium current is involved in the generation of some sleep rhythms (Benington et al., 1995; Vyazovskiy et al., 2002; Espinosa et al., 2004; Cirelli et al., 2005). These studies were not specifically about SWS frequencies (<1 Hz) and thus, no evidence are found to explain how the silent states are initiated. However, some hypothesis suggest that synaptic depression of active synaptic connections (Markram et al., 1997; Tsodyks and Markram, 1997), the slow inactivation of the persistent sodium current (Fleidervish et al., 1996; Fleidervish and Gutnick, 1996), the activation of calcium-dependent potassium current (Schwindt et al., 1992), and the activation of sodium-dependent potassium current (Schwindt et al., 1989), would displace the membrane potential of neurons from the firing level and the entire network would go to the silent state, and these hypothesis were confirmed by modeling studies (Bazhenov et al., 2002; Hill and Tononi, 2005).

There are few studies concerning the mechanism responsible for the initiation of active state. One of them suggest that a small number of cells organized in space would initiate the active state (Cossart et al., 2003). This study was done in slices with ACSF containing 3 mM of potassium and 2 mM of calcium, and these authors used calcium imaging to detect neuronal activity. In this study, only few cells are simultaneously active in few consecutive active periods, and these active periods could last for 60 ms up to 30 s, which is never observed in vivo. In addition, the authors considered an active state when 2 to 3 % of cells were active and there were always active cells (Cossart et al., 2003). In in vivo studies, all neurons recorded are active when the network is active and all neurons recorded are silent when the network is silent (Contreras and Steriade, 1995; Steriade et al., 2001; Timofeev et al., 2001a). Another study, again in slice, suggest that layer 5 IB cells, which are pyramidal neurons, are responsible for the onset of active state (Sanchez-Vives and McCormick, 2000). In this study, the authors used 1.0 to 1.2 mM of calcium and 3.5 mM of potassium in the ACSF which is similar to in vivo conditions. Their slow waves were much more similar to what is seen in vivo than the previous study have shown, but still, they observed spontaneous firing in layer 5 and 6 during silent states, which is not observed in vivo. A third study investigating the origin of active state was done in vivo in cortical slab preparation, a gyrus isolated from thalamic inputs with blood supply preserved (Timofeev et al., 2000b). In this study, the authors observed that the active and silent states were present, which suggest the cortical origin of active state. Some other studies tried to demonstrate that slow oscillation has a cortical origin and one of them showed the presence of slow oscillation after extensive thalamic lesions (Steriade et al., 1993b) and another one showed an absence of slow oscillations in the thalamus of decorticated cats (Timofeev et al., 1996). In cortical slab preparations, the frequency of active state was much slower than in intact cortex, but the larger the isolated gyrus was, the faster was the frequency of active state (Timofeev et al., 2000b). In addition, the authors observed an increase in spontaneous potential before the onset of active state and their conclusion was that the active state onset is due to a summation of spontaneous neuromodulator release.

It is important to point out that like neocortical neurons, neostriatal, thalamic reticular, and thalamocortical neurons are hyperpolarized during silent state (Wilson et al.,

1983; Wilson, 1986; Contreras et al., 1996; Steriade et al., 2001). However, during active state, cortical, neostriatal, and inhibitory thalamic reticular neurons are depolarized and fire spikes while thalamocortical neurons are hyperpolarized with rhythmic inhibitory postsynaptic potential and occasionally fire rebound spike-burst (Contreras and Steriade, 1995; Timofeev and Steriade, 1996). The long lasting hyperpolarisations in cortical neurons are absent when brain cholinergic structures are active (Metherate and Ashe, 1993; Steriade et al., 1993b) or during REM sleep and waking (Steriade et al., 2001; Timofeev et al., 2001a).

Both, the transition from SWS to waking state and the transition from SWS to REM sleep depends on the increase in the activity of neuromodulatory systems (Steriade and McCarley, 1990). During waking state, the level of noradrenaline, serotonin, and acetylcholine are increased while during REM sleep only the level of acetylcholine is increased (Steriade et al., 1997). An increase in the level of activity of neuromodulatory systems increased the input resistance of neurons (Steriade et al., 2000). In vitro data showed that an application of activating neuromodulators increased the input resistance by blocking potassium currents (McCormick, 1992).

In the present thesis, we show that IB cells from any layer tend to be the first to discharge, thus to trigger the active state, but deepest cells tend to lead over superficial ones. In fact, we observed that the active state could be initiated in any layer, but preferentially in deepest layer and that IB cells were the first to be in active state in the vast majority of cycles analyzed.

1.8.2 Delta oscillation

The frequency of sleep delta oscillation is in the range of 1 to 4 Hz. The delta oscillations are different from the slow oscillations (Achermann and Borbely, 1997) since the delta oscillations are attenuated in the transition from the first level of non-REM sleep to the second. In the thalamus, delta oscillations are generated intrinsically in neurons. An interplay of low-threshold calcium current (I_T) and hyperpolarisation activated cation current (I_h) can generate delta oscillation when thalamocortical cells are hyperpolarized, thus during deep sleep (McCormick and Pape, 1990; Leresche et al., 1991; Soltesz et al.,

1991; Dossi et al., 1992). In a single thalamocortical cell, the delta activity is generated by a long-lasting hyperpolarisation, which induce an activation of I_h that depolarizes the cell and activate the I_T which induces rebound burst. Both current are inactivated during burst, I_h is inactivated because of voltage dependence (Pape, 1996) and I_T is inactivated because it is a transient current (Huguenard, 1996) and thus, the cell becomes hyperpolarized after the burst termination, and this initiates the next cycle.

1.8.3 Spindle Oscillation

Sleep spindle oscillations consist of waxing-and-waning field potentials of 7-14 Hz which last 1 to 3 seconds and recur every 5 to 15 seconds (Fuentealba and Steriade, 2005). In vivo, spindle oscillations are observed during early stages of sleep and during the active phases of SWS oscillations. The origin of spindles is known. The spindles are generated in isolated thalamic reticular nucleus (Steriade et al., 1987; Bazhenov et al., 1999) and spindles are absent in the dorsal thalamus that is disconnected from the reticular nucleus (Steriade et al., 1985), which suggests that spindles are generated in the reticular nucleus. The thalamic reticular nucleus is interconnected via GABAergic connection and it was shown that about 30% of thalamic reticular neurons have a prolonged hyperpolarisation before the spindle oscillations (Fuentealba et al., 2004b). The reversal potential of chloride channel, which are opened by GABA via GABAa receptor, is about -70 mV and the resting potential of thalamic reticular cell is about -78 mV (Huguenard, 1996; Fuentealba et al., 2004a; Fuentealba et al., 2005) and thus, the reversed IPSPs could trigger LTSs burst (Bazhenov et al., 1999). These bursts would hyperpolarize thalamocortical neurons and at the end of these IPSPs, thalamocortical neurons would generate rebound spike-burst that excite cortical neurons and thalamic reticular neurons. Then the firing of corticothalamic neurons would contributes to the spindle synchronization via depolarization of both, reticular and thalamocortical neurons. The strong influence of cortical neurons on reticular neurons (Golshani et al., 2001) will excite strongly reticular cells and thus, thalamocortical cell will be hyperpolarized and the next cycle is started. The waning phase would be due to calcium induced cAMP up-regulation of I_h current in thalamocortical cells (Bal and McCormick, 1996; Budde et al., 1997; Luthi et al., 1998) and network desynchronisation (Timofeev et al., 2001b).

1.8.4 Gamma and ripples

During SWS, gamma (30-60Hz) and ripples (>100 Hz) oscillations are observed during the active phase. The ripples were associated with neuronal depolarization and they were more present during active phase of SWS then during waking state or REM sleep (Grenier et al., 2001). A set of cortical and thalamic neurons fire in phase-locked during gamma activities (Steriade et al., 1996a; Steriade et al., 1996b; Timofeev and Steriade, 1997).

Chapter II

2. Article I: Origin of spontaneous active states in local neocortical networks during sleep oscillations

Sylvain Chauvette[1], Maxim Volgushev[2,3], Igor Timofeev[1]
[1] *Department of Anatomy and Physiology, Laval University, Québec, G1K 7P4, Canada*
[2] *Department of Neurophysiology, Ruhr-University Bochum, D-44780, Germany*
[3] *Institute of Higher Nervous Activity and Neurophysiology, Moscow, 117485, Russia*

French Title: Origine des états actifs spontanés dans les réseaux néocorticaux locaux pendant le sommeil

2.1 Résumé

Des alternations spontanées des états actifs et silencieux se produisent pendant le sommeil à ondes lentes. Les causes de la transition de l'état silencieux vers l'état actif demeurent inconnues. Afin d'étudier les mécanismes neuronaux menant aux déclenchements des états actifs, nous avons procédé à des enregistrements multisites simultanés de potentiels de champ et à des enregistrements de l'activité intracellulaire de 2, 3 ou 4 neurones situés près l'un de l'autre chez des chats anesthésiés et chez des chats durant un sommeil naturel (non-anesthésié). Nous avons trouvé que les neurones séparés par des dizaines jusqu'à des centaines de micromètres, n'importe quel des 2 à 4 neurones pouvait être le premier à révéler le déclenchement de l'activité. Le déclenchement des états actifs pouvait être retardé par autant que 100 ms. Les neurones avec décharges en bouffées de potentiels d'action de n'importe quelle couche et les neurones situés profondément avaient tendance à montrer les premiers le déclenchement des états actifs. Nos données supportent l'hypothèse que les états actifs spontanés pouvaient débuter à n'importe quel endroit dans le néocortex.

2.2 Abstract

Spontaneous alternations of active and silent states occur during slow-wave sleep. The causes for the transition from silent to active states remain unknown. To investigate neuronal mechanisms leading to the active states onset we used simultaneously multisite field potential and intracellular activities from 2, 3 or 4 closely located neurons in anesthetized and naturally sleeping cats. We found that in neurons separated by tens to hundred of micrometers any of 2-4 neurons could be the first that reveal the onset of activity in local neuronal groups. The onset of active states could be delayed by as much as 100 ms. Both intrinsically-bursting neurons from any layer and deeply laying neurons had tendency to lead the onset of active states. Our data support the hypothesis that spontaneous active state could start in any place of neocortex.

2.3 Introduction

Spontaneous activity is an emergent property of the cortical network in various states of vigilance that occurs even in the absence of sensory stimuli or any other inputs. The state of sleep (slow-wave sleep) is characterized by the presence of slow EEG waves [1]. During sleep, cortical neurons display alternations of silent and active states, which correspond to depth-positive and depth-negative waves of EEG [2-4]. Human studies have shown that each wave of slow oscillation originates at a definite site, more frequently in prefrontal-orbitofrontal regions and propagate in an anteroposterior direction [5]. Three hypotheses suggest that the basis of active states is (a) spontaneous mediator release in a large population of neurons leading to occasional summation and firing [6], (b) spontaneous intrinsic activity in layer 5 intrinsically bursting neurons [7] and (c) the selective synchronization of spatially structured neuronal ensembles involving a small number of cells [8].To resolve such contradictory conclusions on the origin of active network states we performed multisite local field potential and intracellular recording followed by staining in anesthetized and non-anesthetized cats. Here we show that active network states could start from any cortical area and at any depth, but the leading role in the onset of active states is played by deeply laying neurons.

2.4 Database

We recorded intracellular activities from 16 anesthetized and 2 non anesthetized cats with the aim to obtain multisite (16 channels) field potential recordings from different cortical depth by mean of Michigan probes or dual, triple or quadruple intracellular recordings from cortical neurons. The medio-lateral/antero-posterior distance between 4 intracellular electrodes was <0.3 mm (usually 0.1 mm) (Fig. 1 a, b). In these experiments we obtained 4 quadruple, 3 triple and 28 dual recordings from anesthetized and 5 dual intracellular recordings from naturally sleeping cats.

2.5 Results

Most of the neurons recorded in anesthetized animals were electrophysiologically identified [9-11]. Because the responses of the same neuron to depolarizing current pulses change depending on the state of the network [12,13], we applied depolarizing current pulses eliciting action potentials with at least 3 intensities and the same current pulse was applied at least 10 times. If the response to one of the current pulses was different from Regular-Spiking (RS) pattern we classify this neuron according to the response to this current pulse. 71 out of 81 neurons recorded in the present study in anesthetized animals were electrophysiologically identified as RS, (71.8 %), Fast-Rhythmic-Bursting (FRB, 16.9 %), Intrinsically-Bursting (IB, 8.5 %) and Fast-spiking (FS, 2.8 %).

Local field potential recordings. Under Ketamine-Xylazine anesthesia, the EEG displays a slow oscillation (Fig. 1) that is similar to the slow oscillation occurring during natural slow-wave sleep (Fig. 2). In order to determine the origin of the active state, we recorded 15 local field potentials (LFP) with a Michigan probe inserted perpendicularly to the neocortex surface. The transitions from depth-positive/surface-negative (silent) state to depth-negative/surface-positive (active) states were fitted with a sigmoid curve to eliminate impact of noise and the time at 10% of the transition amplitude was taken as the onset of active state (Fig. 1 a). A high variability in activation order was observed and any of electrodes could be the first one to display the transition from silent to active states. The longer the interelectrode distance, the higher the degree of variability in activation time was seen (compare EEG 2-1 with EEG 8-1 in Fig. 1 b). However, the deep electrodes showed a tendency to be activated first (Fig. 1b and c).

To further investigate the location of the onset of active state, we recorded 16 LFP with a Michigan probe inserted perpendicularly to the neocortex surface during natural sleep and computed current-source density maps from these recordings (Fig. 2). In order to reduce the influence of high EEG frequencies in the current-source density analysis, we filtered offline the LFP between 0.5 and 6 Hz. The current-source density maps showed the

presence of a source during the depth-positive EEG waves located in channels 9 and 11 (corresponding depth are 900 and 1100 μm respectively) (Fig. 2 b). Since the depth-positive EEG waves correspond to the periods of disfacilitation [3], the presence of source indicate that excitatory activity was reduced primarily at that depth. The borders of source at this depth (10 % of transition, white lines on Fig. 2 b and c) indicate that the onsets of active states started here. This pattern of activity was found in the majority of cases (86 %). The current-source density analysis of an average of 50 cycles emphasized the presence of source in channels 9 and 11 and also showed a major sink in channels 3-5 and 10.

In order to study the cellular mechanisms of the active state onsets, we made quadruple, triple, and dual intracellular recordings from closely located neurons (Fig. 3). The recorded cells were electrophysiologically identified as previously described (Fig. 3, d). The lateral distance between recorded pipettes was usually around 100 μm and never exceeded 300 μm. On a coarse time scale, onsets of active and silent states occurred at about the same time in all closely located neurons recorded at any depth. To quantify the timing of the active state onset, we fitted the transitions from silent to active states with a sigmoidal curve and the time at 10% amplitude was taken as the time for onset of active state. On the fine time scale, the onsets of active states were not simultaneous and the order of involvement of neurons in activity was not uniform, but varied from one cycle to the other. Any cell could be leading in some cycles, but followed other cells in other cycles (Fig. 3, c, e). However, there was a clear tendency for particular neurons either to be leading or following other neurons. In the example shown in the Fig. 3, the deeply laying FRB neuron (green) was taken a reference. The blue intrinsically bursting neuron lying at a depth of about 950 μm had strong tendency to lead and a regular-spiking neuron lying at the same depth had tendency to follow as shown in histograms of active state onset delays (Fig. 3, e).

We compared the depth distribution of leading neurons in all recorded neuronal pairs (Fig. 4, a). The maximum of Gaussian fitting of delay distribution was taken as characteristic delay of the onset for this cell (Fig. 3 f). The more superficially located neurons were leading in only 16 % of cases (Fig. 4, a, left), the deeply located neurons were

leading in 38% of cases (Fig. 4, a, middle) in the other cases the depth of recorded neurons was similar (less than 200 μm from manipulator reading, Fig. 4, a, right). Thus, in agreement with field potential recordings, the neurons located in deeper layers had tendency to lead the onsets of active states. The averaged delay of active state onset was 7.6 ± 6.8 ms (range: 0.3 to 35.9 ms, n = 53, Fig. 4 b) while the averaged standard deviation of delays was 16.1 ± 4.4 ms (range: 8.8 to 28.2 ms, n = 53, Fig. 4, c) suggesting large variability of the activity onsets in different cycles.

Next, we wondered if active states originated earlier in neurons of a particular electrophysiological class. All electrophysiological types of neurons were distributed throughout all cortical layers (Fig. 5 a). Two types of comparison were made. First, we compared the leading ability of a particular neuron on the basis of mean maxima of delay histograms (Fig. 5, b), and then we compared the leading ability of a particular neuron on a cycle-by-cycle basis. The IB neurons were leading in all IB/RS pairs (n = 5) and in 76.4% of the 210 cycles analyzed for this pair type (range 60% to 88%). In 4 IB/FRB pairs, the IB led in three pairs and led in 57.1 % of the 182 cycles analyzed (range 40% to 69%). In the only pair where the FRB led the IB neuron, which is shown in figure 3, the IB neuron was located much more superficially than the FRB cell. Out of 9 FRB/RS pairs, the FRB led in 7 pairs and in 58.2% of the 544 analyzed cycles (range 35% to 87%). We recorded only 2 FS cell in this study, one FS/RS pair and one FRB/FS pair. In both cases, on the histogram of leading neuron distribution the FS neuron was led by other neurons (not shown).

We used also a second approach to detect the active and the silent states (Fig. 6). We calculated the mean membrane potential and its SD in a running window of 25 ms, and plotted a 3D distribution of the occurrence of pairs of mean and SD values (Fig. 6 c, d). Silent states formed a sharp peak at hyperpolarized potentials and low SD values. Active states are represented in this plot by a broader hill at more depolarized potentials and higher SD values. Since the peak location differs along both axes, the use of a combination of these two parameters allows the detection and separation of the states (Fig. 6 c, d). To eliminate the impact of brief spontaneous fluctuations of the membrane potential the periods lasting less than 40 ms were not considered for further analysis. A typical example

of the active state transition for these 4 neurons is shown in the figure 6, b1, in which the earlier onset was observed in the deepest cell, and systematically increase in more superficially recorded cells. Figure 6, b2 shows an example of a very different sequence of activity, with the cell 3 leading and the other 3 cells following with some delay.

To quantify the timing of the active states onset in a given neuron, the mean time of the active state onsets in a combination of 2, 3 or 4 neurons was considered as 0 time, and the delays from this time were plotted against the depth of the cortex (Fig. 7). Similar to identification with onsets of activities (Figs. 3-4) the depth distribution of delays demonstrated that the neurons lying in deep layers had tendency to lead the active states. To make quantitative analysis we averaged times of the transition for upper layers (0-0.7 mm), middle layers (0.7-1.4) mm and deep layers (1.4 mm and below). The transition from silent to active states in the deep layer preceded the middle and upper layers by more than 4 ms (Fig. 7, a). The transitions to silent states did not reveal any constant propagation observed in any neuronal group (Fig. 7, c). Similar to the onsets of active states (Fig. 5, c) the IB neurons were leading in the transition to the active states (Fig. 7, b), and there was no special neuronal type leading the transition to the silent states (Fig. 7, d).

To verify whether the cycle-to-cycle variability in onsets of active states exists also during natural sleep, we performed dual intracellular recordings in non-anesthetized and non-paralyzed cats (Fig. 8). Similar to previous studies both waking and REM sleep were characterized by activated EEG pattern and the neurons remained in active state for the duration of these behavioral conditions. The bimodal membrane potential distribution was found only during periods of slow-wave sleep. In 5 paired recordings we found that similar to anesthetized animals the onsets of active states could occur (1) in any neuron, (2) in each neuronal pair there was a neuron that had tendency to lead and (3) the delays in onset fluctuation in a given neuronal pair were reaching 40 ms.

2.6 Discussion

Here we investigated whether there is a particular group of neurons that drives the onsets of active states. Both local field potential and intracellular data demonstrate that any cortical layer could drive a particular cycle of the active state. However in the majority of cases the active states originate from deep cortical layers. In addition, we found that IB neurons from any cortical layer have tendency to be the first to generate the active state onsets.

The slow oscillation represented by alternations of active and silent states[14] has cortical origin. This conclusion is based on two lines of evidence: (a) the slow oscillation was observed in athalamic animals [15] and other isolated cortical preparations [7,16], but is absent in the thalamus of decorticated animals [6]. Two of the previous studies on the subject suggested a particular role of IB neurons in the generation of active states [7,16]. It is clear that the bursts generated by these neurons could have major postsynaptic impact and thus involve other neurons in the active state [16,17]. Since in the neocortex the silent states are also associated with higher extracellular Ca^{2+} concentration [18,19] the release probability should be higher, facilitating synaptic propagation of active states. Calcium imaging study in vitro also demonstrated that activity could start from any neuronal group [8], however, likely due to the destruction of neuronal connections in the slice [20,21], once started, the activity did not involve all neighboring neurons. In another slice preparation [7], the active periods were elicited by spontaneous firing of layer V-VI neurons. Again, very likely due to the connectivity issues, the active states were not elicited when the firing of layer V-VI neurons started, but only after some period of time. Thus the period of slow oscillation recorded in that preparation was much longer as compare to in vivo recordings from both anesthetized and sleeping animals. In the present experiments as well as in other in vivo studies [2-4] no neurons fired during silent network states.

The critical question is what drives the first neuron to generate first spike leading to the onset of active period? Two major mechanisms are possible. The first ones relies on intrinsic properties of a particular group of neurons in which, due to specific channel,

neurons generate spontaneous action potentials, the second possibility relies on synaptic potentials that could drive the active states.

Most of known intrinsic currents that could maintain prolonged depolarizing state should be driven by some input signals [22,23]. The only current that at approximately resting membrane potential could generate oscillatory behavior is hyperpolarisation activated depolarizing current (Ih) [24]. However, the strength of this current in cortical neurons is relatively weak, and cannot lead to spontaneous firing like it does in the thalamus.

The onsets of active states occur when all cortical neurons are silent. During silent states the only synaptic events that could occur are those due to spontaneous, spike independent release [16,25,26]. The frequency of miniature synaptic events increases with increase in the probability of evoked release [27]. Since the evoked release probability increases toward the end of silent state [19] they are the good candidates to drive the active states. Because any synapse could spontaneously release mediator, than any neuron could be excited first. The probability of spontaneous excitation due to the presence of minis should grow with the increase number of synapses. The number of spines on thick layer 5 pyramidal cells is larger than the number of spines on any other type of neurons [28]. This indicate that the mini driven activity would likely start first in these neurons. The axons of layer V neurons ramify primarily in layer V and VI, sending only weak connections to layer II-III [29]. Cortico-cortical layer VI neurons provide long-range, phasic excitatory input to other infragranular pyramidal cells [30] and highly effective inputs to layer IV [31,32]. From layer IV the activity is effectively distributed to layers II-III as well as to layers V-VI [29].

Thus our study demonstrated that deeply lying neurons lead the onsets of active states. This conclusion is supported by their morphological features and connectivity properties. Some of these neurons are intrinsically bursting [33]. Their burst firing allows significant amplification of low amplitude signals at target structures and their postsynaptic impact is strong enough to induce activity. Since any neuron could induce activity the leading role of IB neurons is only probabilistic and not determinative.

2.7 Method

2.7.1 Preparation

Experiments in anesthetized animals. Acute experiments were carried out on 16 adult cats of both sexes that had been anesthetized with ketamine and xylazine (10-15 and 2-3 mg/kg i.m., respectively). All pressure points and the tissues to be incised were infiltrated with lidocaine (0.5%). The animals were paralyzed with gallamine triethiodide and artificially ventilated, maintaining the end-tidal CO_2 concentration at 3.5-3.8%. A permanent sleep-like state, as ascertained by continuous recording of the EEG, was maintained throughout the experiments by administering additional doses of ketamine (5 mg/kg). The body temperature was monitored by a rectal probe and maintained at 37oC via a feedback-controlled heating pad. The heart rate was continuously monitored (90-110 beats/min). The stability of intracellular recordings was ensured by cisternal drainage, bilateral pneumothorax, hip suspension and by filling the hole made for recordings with a solution of 4% agar.

Experiments in non-anesthetized animals. Experiments on non-anesthetized animals were conducted on 2 adult cats, chronically implanted as previously described [2,3]. Briefly, surgical procedures for chronic implantation of recording and stimulating electrodes were carried out under deep barbiturate anesthesia (Somnotol, 35 mg/kg, i.p.), followed by two to three administrations, every 12 h, of buprenorphine (0.03 mg/kg, i.m.) to prevent pain. Penicillin (500,000 units i.m.) was injected during three consecutive days. During surgery, the cats were implanted with electrodes for electro-oculogram (EOG), electromyogram (EMG) from neck muscles, and intracortical EEG recordings. In addition, one chamber allowing the intracellular penetrations of micropipettes was placed over neocortical areas 5 and 7. Acrylic dental cement was used to fix on the skull the electrodes and recording chamber.

At the end of experiments, the cats were given a lethal dose of pentobarbital (50 mg/kg i.v.).

2.7.2 Recording

Local field potentials were recorded in the vicinity of impaled neurons and also from more distant sites, using either tungsten electrodes (10-12 MΩ) or 16 channels Michigan probe inserted perpendicularly to the surface in neocortical areas 5, 7 or 21. Dual, triple or quadruple intracellular recordings from suprasylvian association areas 5 and 7 were performed using glass micropipettes filled with a solution of 3 M potassium-acetate (KAc). A high-impedance amplifier with active bridge circuitry was used to record the membrane potential and inject current into the neurons. All electrical signals were sampled at 20 kHz and digitally stored on Vision (Nicolet, Wisconsin, USA). Offline computer analysis of electrographic recordings was done with IgorPro software (Lake Oswego, Oregon, USA) and with custom written MatLab programs. At the end of experiments, the cats were given a lethal dose of pentobarbital (50 mg/kg i.v.).

2.7.3 Analysis

A sigmoidal curve fitting was performed on the transition between silent and active state (Fig. 1 and 3). The onset of the active state was defined as the time at which the amplitude between the silent and active state reached 10% level. A reference channel was chosen arbitrarily and the time at ten percent of amplitude for each other electrode was then compared to this reference. These values were compiled for every cycle to produce delay histograms (Figs. 1 and 3).

For current-source density (CSD) analysis, the local field potentials were filtered between 0.5 and 6 Hz to eliminate the influence of other rhythm in the analysis. According to original description [34,35], we used the following formula to do CSD analysis:

$$-Im = (1/R) * ((\Phi 3 - 2\,\Phi 2 + \Phi 1) / (Z2))$$

where

Φ = field potential in mV

R = in MOhms

Z = distance between electrodes in mm

Im = CSD in mV/mm2

For:

Im > 0 Source => outward current

Im < 0 Sink => inward current

2.8 References

1. Blake, H. & Gerard, R. W. Brain potentials during sleep. Am J Physiol 119, 692-703 (1937).
2. Steriade, M., Timofeev, I. & Grenier, F. Natural waking and sleep states: a view from inside neocortical neurons. J Neurophysiol 85, 1969-85 (2001).
3. Timofeev, I., Grenier, F. & Steriade, M. Disfacilitation and active inhibition in the neocortex during the natural sleep-wake cycle: An intracellular study. Proc Natl Acad Sci U S A 98, 1924-1929 (2001).
4. Contreras, D. & Steriade, M. Cellular basis of EEG slow rhythms: a study of dynamic corticothalamic relationships. J Neurosci 15, 604-22 (1995).
5. Massimini, M., Huber, R., Ferrarelli, F., Hill, S. & Tononi, G. The sleep slow oscillation as a traveling wave. J Neurosci 24, 6862-70 (2004).
6. Timofeev, I. & Steriade, M. Low-frequency rhythms in the thalamus of intact-cortex and decorticated cats. J Neurophysiol 76, 4152-68 (1996).
7. Sanchez-Vives, M. V. & McCormick, D. A. Cellular and network mechanisms of rhythmic recurrent activity in neocortex. Nat Neurosci 3, 1027-34 (2000).
8. Cossart, R., Aronov, D. & Yuste, R. Attractor dynamics of network UP states in the neocortex. Nature 423, 283-8 (2003).
9. Connors, B. W. & Gutnick, M. J. Intrinsic firing patterns of divers neocortical neurons. Trends Neurosci 13, 99-104 (1990).
10. Steriade, M. & Amzica, F. Dynamic coupling among neocortical neurons during evoked and spontaneous spike-wave seizure activity. J Neurophysiol 72, 2051-69 (1994).
11. Gray, C. M. & McCormick, D. A. Chattering cells: superficial pyramidal neurons contributing to the generation of synchronous oscillations in the visual cortex. Science 274, 109-113 (1996).
12. Steriade, M. Neocortical cell classes are flexible entities. Nat Rev Neurosci 5, 121-34 (2004).
13. Steriade, M., Timofeev, I., Dürmüller, N. & Grenier, F. Dynamic properties of corticothalamic neurons and local cortical interneurons generating fast rhythmic (30-40 Hz) spike bursts. J Neurophysiol 79, 483-90 (1998).
14. Steriade, M., Nuñez, A. & Amzica, F. A novel slow (<1 Hz) oscillation of neocortical neurons in vivo : depolarizing and hyperpolarizing components. J Neurosci 13, 3252-3265 (1993).
15. Steriade, M., Nuñez, A. & Amzica, F. Intracellular analysis of relations between the slow (<1 Hz) neocortical oscillations and other sleep rhythms of electroencephalogram. J Neurosci 13, 3266-3283 (1993).
16. Timofeev, I., Grenier, F., Bazhenov, M., Sejnowski, T. J. & Steriade, M. Origin of slow cortical oscillations in deafferented cortical slabs. Cereb Cortex 10, 1185-1199 (2000).
17. Lisman, J. E. Bursts as a unit of neural information: making unreliable synapses reliable. Trends Neurosci 20, 38-43 (1997).
18. Massimini, M. & Amzica, F. Extracellular calcium fluctuations and intracellular potentials in the cortex during the slow sleep oscillation. J Neurophysiol 85, 1346-50. (2001).

19. Crochet, S., Chauvette, S., Boucetta, S. & Timofeev, I. Modulation of synaptic transmission in neocortex by network activities. Eur J Neurosci 21, 1030-1044 (2005).
20. Thomson, A. M. Activity-dependent properties of synaptic transmission at two classes of connections made by rat neocortical pyramidal axons in vitro. J Physiol 502, 131-147 (1997).
21. Thomson, A. M. & Deuchars, J. Synaptic interactions in neocortical local circuits: dual intracellular recordings in vitro. Cereb Cortex 7, 510-22 (1997).
22. Fleidervish, I. A. & Gutnick, M. J. Kinetics of slow inactivation of persistent sodium current in layer V neurons of mouse neocortical slices. J Neurophysiol 76, 2125-30 (1996).
23. Pedroarena, C. & Llinás, R. Dendritic calcium conductances generate high-frequency oscillation in thalamocortical neurons. Proc Natl Acad Sci U S A 94, 724-728 (1997).
24. McCormick, D. A. & Pape, H. C. Properties of a hyperpolarization-activated cation current and its role in rhythmic oscillation in thalamic relay neurons. J Physiol 431, 291-318 (1990).
25. Salin, P. A. & Prince, D. A. Spontaneous GABAA receptor-mediated inhibitory currents in adult rat somatosensory cortex. J Neurophysiol 75, 1573-88 (1996).
26. Paré, D., Lebel, E. & Lang, E. J. Differential impact of miniature synaptic potentials on the soma and dendrites of pyramidal neurons in vivo. J Neurophysiol 78, 1735-9 (1997).
27. Prange, O. & Murphy, T. H. Correlation of miniature synaptic activity and evoked release probability in cultures of cortical neurons. J Neurosci 19, 6427-6438 (1999).
28. DeFelipe, J. & Farinas, I. The pyramidal neuron of the cerebral cortex: morphological and chemical characteristics of the synaptic inputs. Prog Neurobiol 39, 563-607 (1992).
29. Thomson, A. M. & Bannister, A. P. Interlaminar connections in the neocortex. Cereb Cortex 13, 5-14 (2003).
30. Mercer, A. et al. Excitatory connections made by presynaptic cortico-cortical pyramidal cells in layer 6 of the neocortex. Cereb Cortex 15, 1485-1496 (2005).
31. Gilbert, C. D. & Wiesel, T. N. Morphology and intracortical projections of functionally characterized neurons in the cat visual cortex. Nature 280, 120-5 (1979).
32. Tarczy-Hornoch, K., Martin, K. A., Stratford, K. J. & Jack, J. J. Intracortical excitation of spiny neurons in layer 4 of cat striate cortex in vitro. Cereb Cortex 9, 833-43 (1999).
33. McCormick, D. A., Connors, B. W., Lighthall, J. W. & Prince, D. A. Comparative electrophysiology of pyramidal and sparsely spiny stellate neurons of the neocortex. J Neurophysiol 54, 782-806 (1985).
34. Mitzdorf, U. & Singer, W. Prominent excitatory pathways in the cat visual cortex (A 17 and A 18): a current source density analysis of electrically evoked potentials. Exp Brain Res 33, 371-94 (1978).
35. Mitzdorf, U. Current source-density method and application in cat cerebral cortex: investigation of evoked potentials and EEG phenomena. Physiol Rev 65, 37-100 (1985).

2.9 Figures legend

Fig. 1. Deep layers have tendency to lead the onsets of active states. a. 15 field potentials recorded with a Michigan probe inserted perpendicularly to the neocortex surface in a cat anesthetized with ketamine-xylazine, EEG 1 is at surface and EEG 15 is the deepest electrode. One cycle is expended as indicated. Sigmoidal fitting of the onsets of active states was performed to eliminate the impact of noise. Ten percent change in the amplitude of the field potential (indicated by vertical lines was tentatively used to indicate the onset of active states. b. 4 Examples of delay histograms and Gaussian fitting (onset in EEG 1 is the reference) c. Peri-event histogram of Gaussian fitting of delays. Note the high variability of delays for electrodes located farther from reference.

Fig. 2. The source of activity is located in deep layers. a. 16 field potentials recorded by means of Michigan probe in non-anesthetized animal during slow-wave sleep and filtered between 0.5 and 6 Hz. EEG 1 is at the surface and EEG 16 is the deepest electrode. b. Current-Source Map analysis. Upper black trace is EEG 1 and lower black trace is EEG 16. White traces represent a 10% transition. Note that the source is mainly located in deep electrodes. c. Current-Source Map analysis of an averaged cycle (n=50).

Fig. 3. In local neuronal constellations the onset of active states occurs in any order. a. Microphotograph of neurons recorded simultaneously and b. their 3-D reconstructions. The color code in b-e is the same and the depth of cells is indicated in b. The grey neuron was recorded before the same electrode as the red neuron, but several minutes prior to the displayed period. c. Simultaneous intracellular recordings from the neurons shown in a and b. Sigmoidal fitting of the onsets of active states was performed to eliminate the impact of noise. d. Histograms of delays of active states order, cell 2 has been arbitrarily chosen as reference. Note the negative shift in the peak of the curve fitting of Cell 3, indicating that cell 3, an IB cell, has tendency to lead in the majority of cycles and also note the positive shift of histogram for cell 1, the RS cell, indicating that it is often the last cell that is involved in the onset of active states. e. 2 expanded examples of from panel c, vertical bars indicate time at 10% amplitude. Note that the onset of activity in different neurons occurs in variable order. f. Electrophysiological identification of neurons shown in (a, b, c).

Fig. 4. In a local network, deeper neurons are leading. a. Plot of relation between depth and mean delay of active state onsets. Each neuron is represented by a dot. Pairs of neurons are linked by a line. Left panel shows cases where the more superficial neuron in the pair was leading, the middle panel represent cases where the deeper neuron of the pair was leading. Right panel shows cases where both neurons were recorded at similar depth (less than 200 μm). Note that the number of leading deeply laying neurons outnumbers the number of superficially laying leading neurons. b. Histograms of delays of active state onsets X-axis is average delay of a pair, y-axis is the percentage of cell pairs. c. Onset delays and standard deviation of onset delays for all data. Note the high standard deviation.

Fig. 5. Intrinsically-bursting neurons initiate active periods. a. A Depth distribution of electrophysiological types of neurons in neocortex. Note that neurons that belong to different electrophysiological types are evenly distributed in all layers of the cortex. b. A percentage of different electrophysiological type of neurons that led the majority of slow wave cycles in a given pair. Note that IB neurons were leading in the vast majority of cases. For IB vs RS, n= 5 pairs; IB vs FRB, n= 4 pairs; FRB vs RS, n= 9 pairs. c. A percentage of cycles led by one electrophysiological type of neurons in a given neuronal pair. IB neurons were leading in the vast majority of cycles. For IB vs RS, n= 210 cycles; IB vs FRB, n= 182 cycles; FRB vs RS, n= 544 cycles.

Fig. 6. Detection of transition between states. a. Simultaneously recorded LFP and intracellular activity of 4 cells in the neocortex. Recording depth is indicated next to each trace. Below each trace, periods of active (green) and silent (red) states are indicated. b1, b2: Expanded view of the periods indicated by grey bars 1 and 2 in a. Vertical dotted line marks the onset of the active state in the leading cell. c,d: Detection of active and silent states. 3D density distribution of the data from a, cell 4. Side view (c) and top view (d). The mean membrane potential and its standard deviation (SD) were calculated in a running window of 25 ms. These values were used as X and Y coordinates; the Z axis is the frequency of their occurrence. Silent states are represented by the peak at low membrane potential and low SD values. Active states are represented by a broader hill at more depolarized membrane potentials and higher SD values. The rightmost cloud of points

represents windows with action potentials. The regions used for detection of active (green) and silent (red) states are outlined in the top view (d).

Fig. 7. Population analysis of the silent-active state transitions in simultaneously recorded neurons. a, c. Dependence of the transition delays in active (a) and silent (c) states on recording depth. For calculation of averages, cells recorded at depth <700 μm, between 701 and 1400 μm, and deeper than 1401 μm were segregated in 3 groups. b,d. Dependence of the transition delays in active (b) and silent (d) states on the cell type. Cells were classified by their intrinsic membrane properties as regular spiking (RS), fast rhythmic bursting (FRB), intrinsically bursting (IB) or fast spiking (FS). UN - unidentified neurons. In a-d, each diamond symbol represents data for one cell; Group averages (circles) are shown with ±SD (bars).

Fig. 8. The high variability in the cell activation order is also present in natural sleep. a. Period of simultaneous dual intracellular recording and DC field that are closely located (<100 μm in lateral distance). b. 2 cycles expanded showing that each neuron can lead a particular cycle. Vertical bars represent the 10% of transition amplitude. c. Histograms of delays of activation. Note the high variability in order of activation (± 40 ms).

2.10 Figures

Figure II- 1

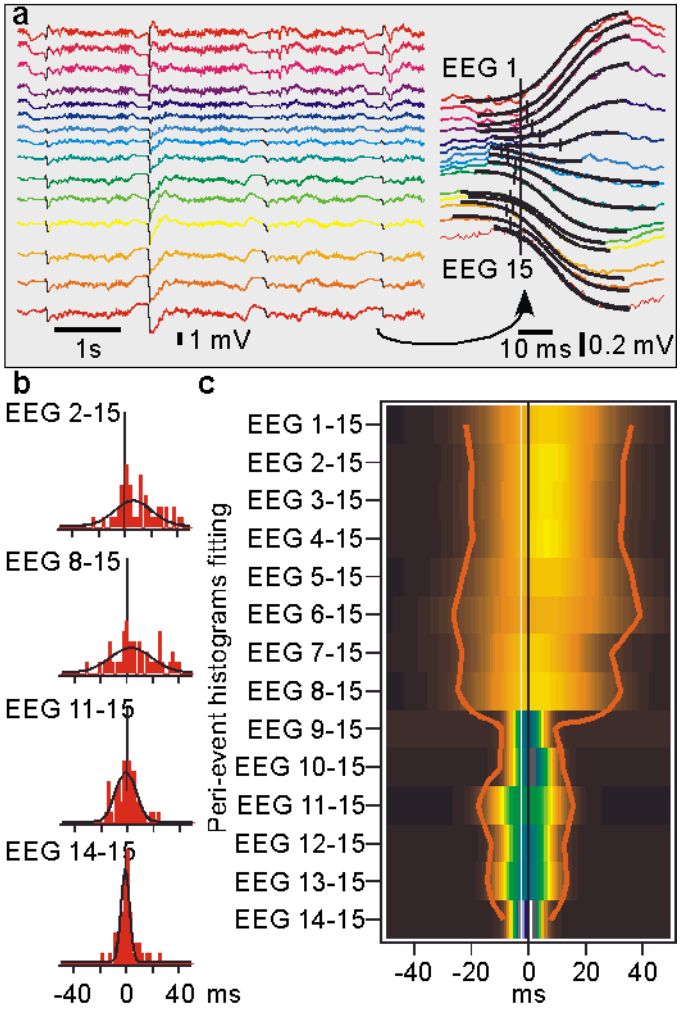

Figure 1

Figure II- 2

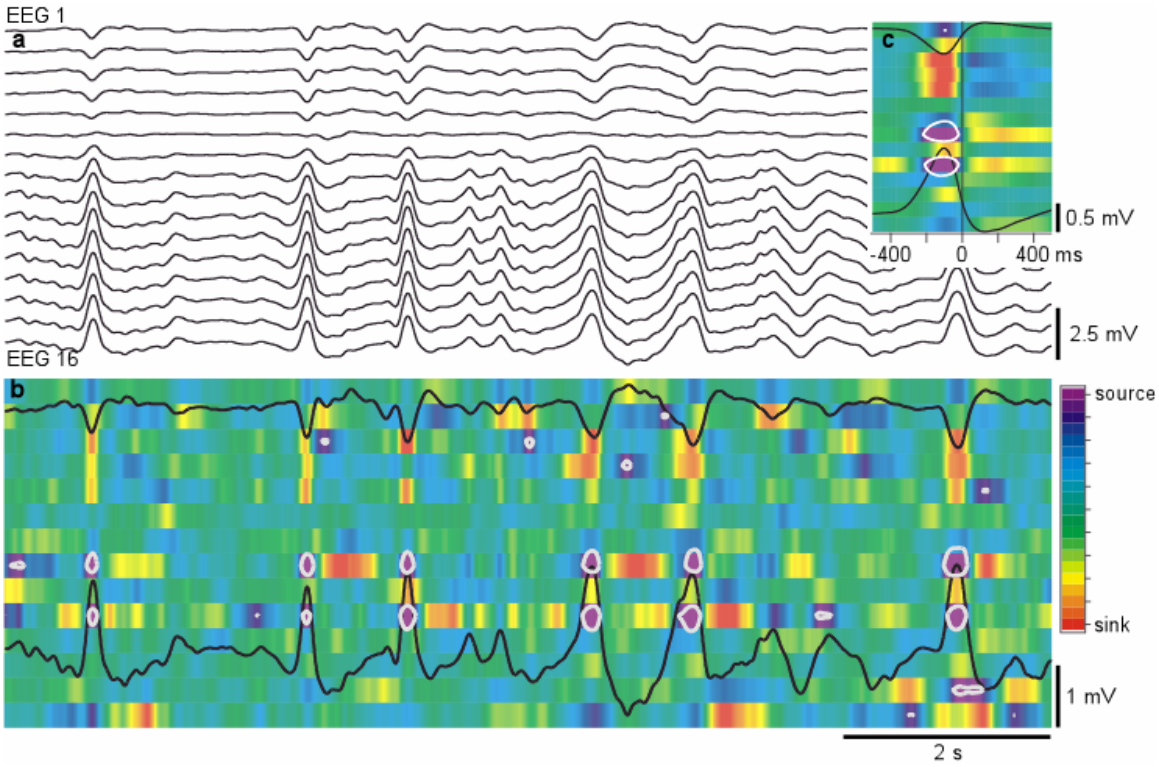

Figure 2

Figure II- 3

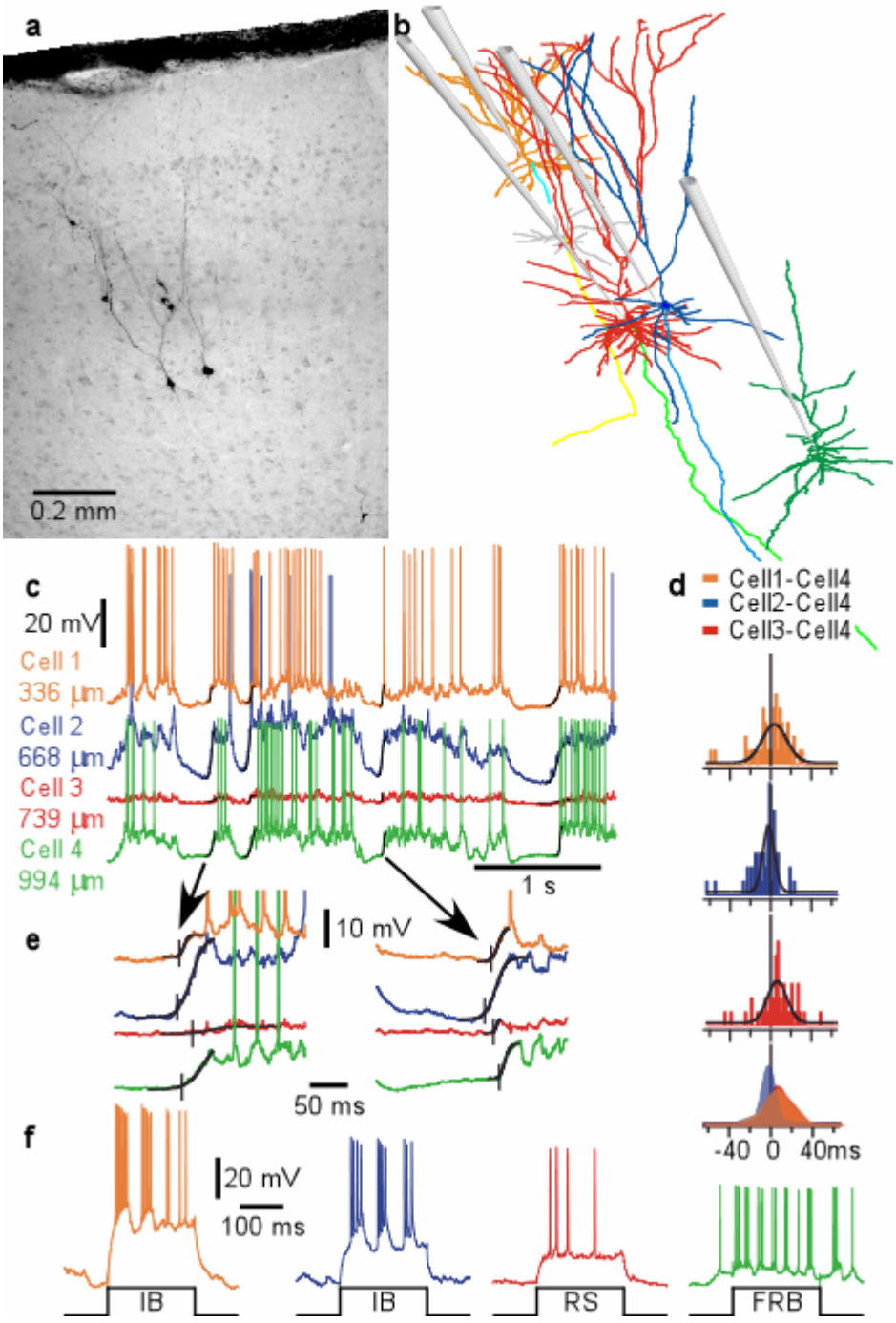

Figure 3

Figure II- 4

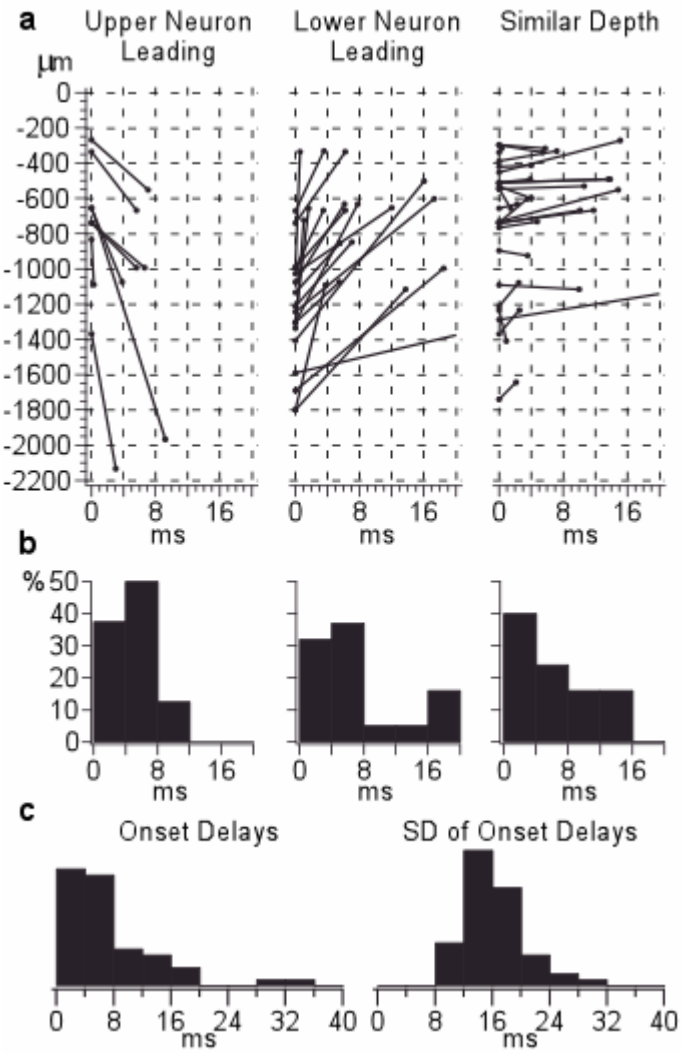

Figure 4

Figure II- 5

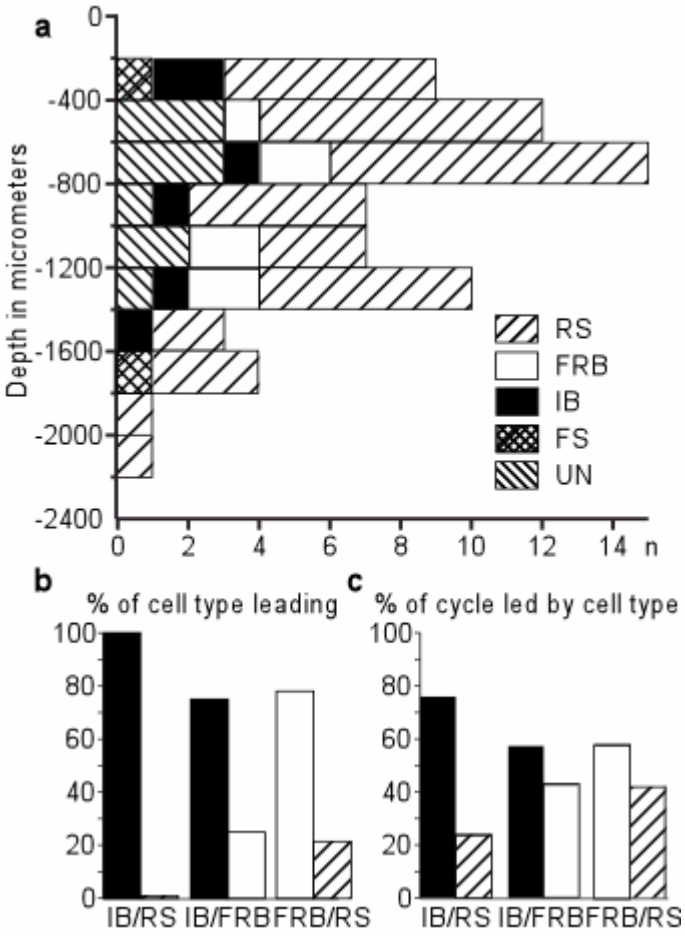

Figure 5

Figure II- 6

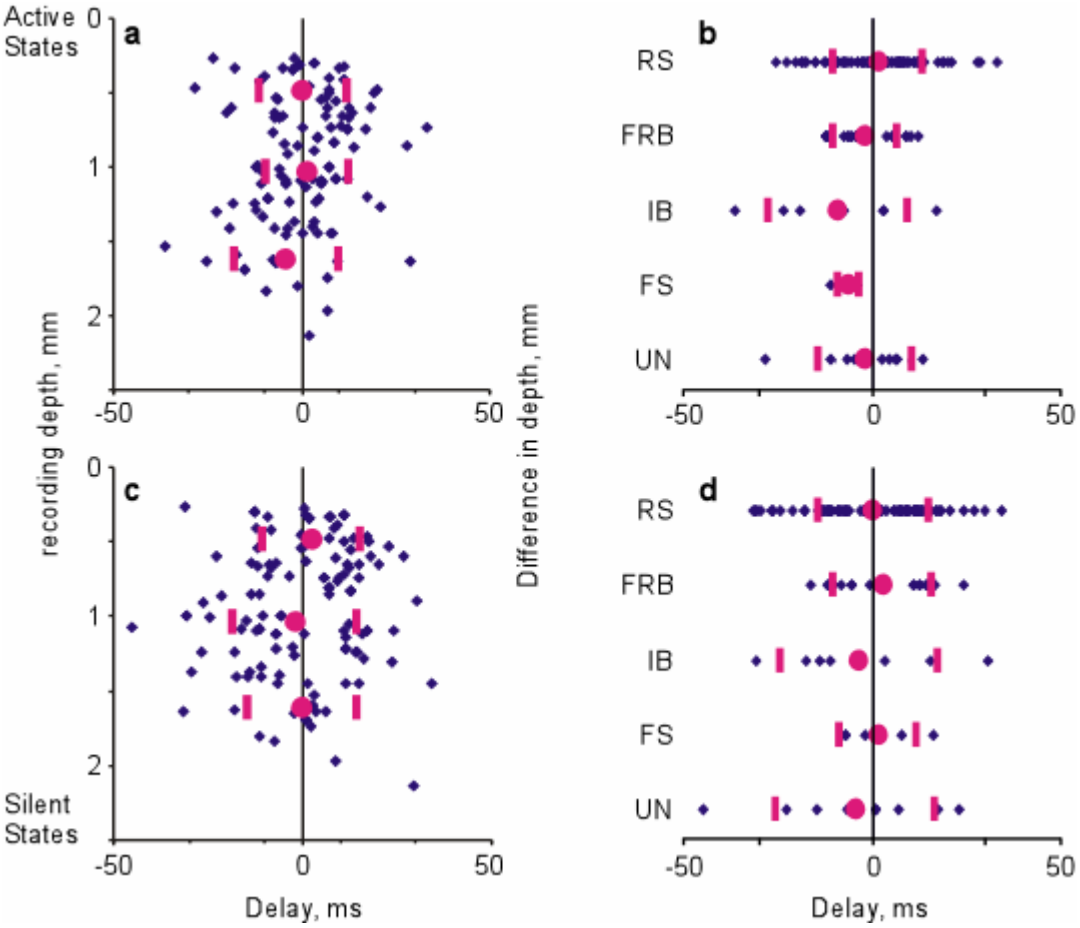

Figure 6

Figure II- 7

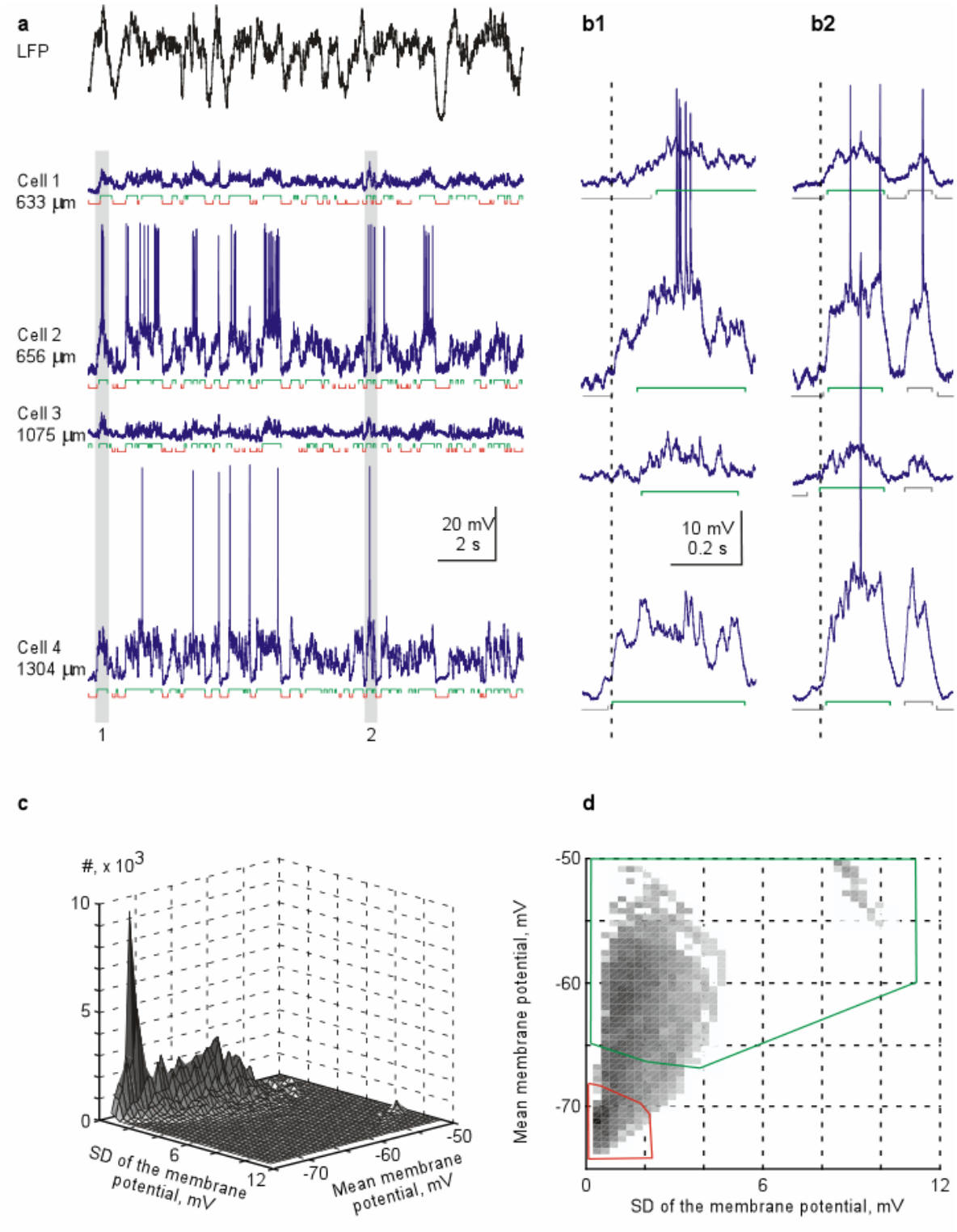

Figure 7

Figure II- 8

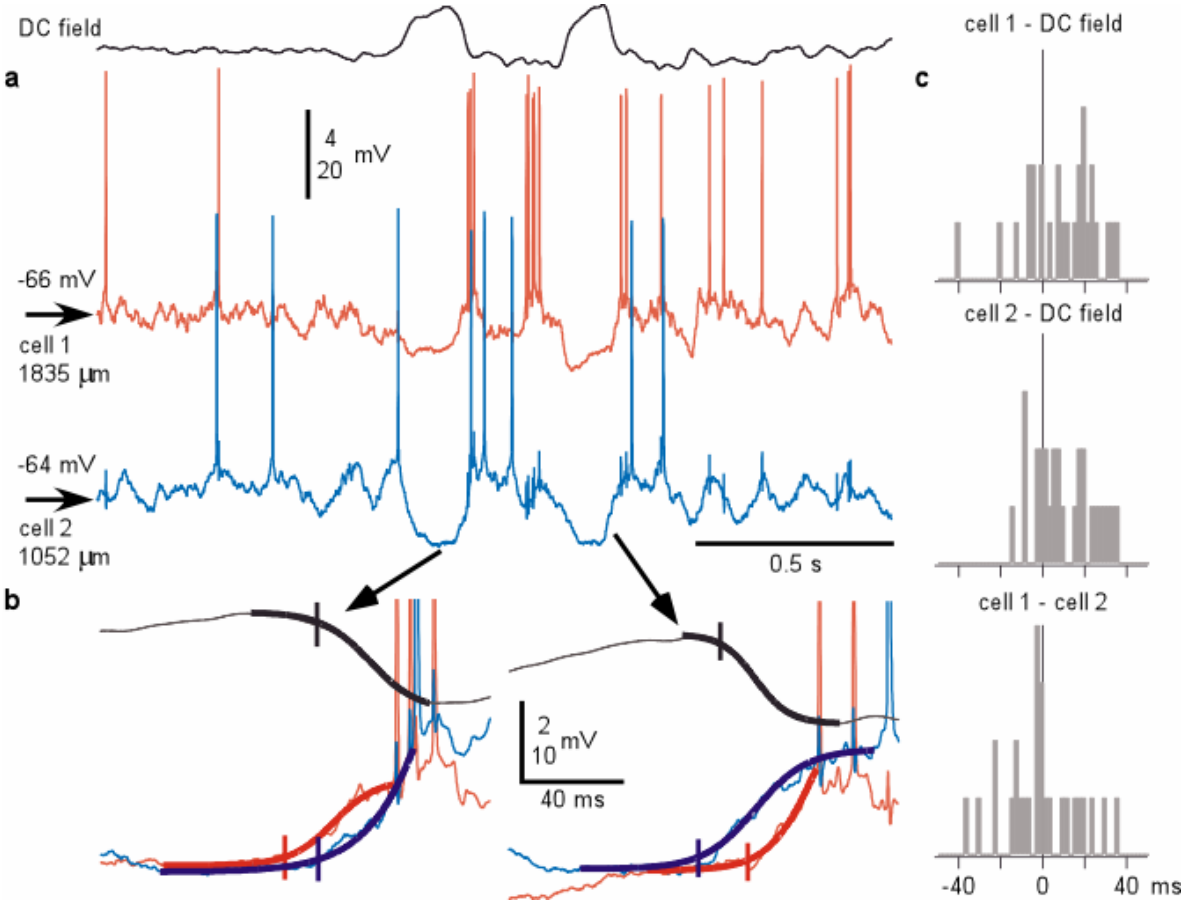

Figure 8

Chapter III

3. Article II: Precise long-range synchronization of activity and silence in neocortical neurons

Sylvain Chauvette[3], Maxim Volgushev[1,2], Mikhail Mukovski[1], Igor Timofeev[3]
[1]*Department of Neurophysiology, Ruhr-University Bochum, D-44780, Germany*
[2]*Institute of Higher Nervous Activity and Neurophysiology, Moscow, 117485, Russia*
[3]*Department of Anatomy and Physiology, Laval University, Québec, G1K 7P4, Canada*

French Title: Synchronisation précise à grandes distances de l'activité et du silence dans les neurones néocorticaux.

Classification: BIOLOGICAL SCIENCES, Neuroscience

Corresponding author:

Igor Timofeev
Department of Anatomy and Physiology
Laval University
Québec, G1K 7P4, Canada
E-mail: Igor.Timofeev@phs.ulaval.ca
Phone: 1 418 656 5166
Fax: 1 418 656 7898

Manuscript information: 18 text pages; 4 Figures; no Tables

Word and character counts: 249 words in the Abstract; 46045 characters in the paper (including figures) plus 9735 characters in supplementary on line material.

Abbreviations:

EEG - electroencephalogram

FRB - fast-rhythmic-bursting cell

FS - fast-spiking cell

IB - intrinsic-bursting cell

LFP - local field potential

RS - regular-spiking cell

3.1 Résumé

Le sommeil à ondes lentes est caractérisé par des alternances entre les périodes actives et silencieuses dans le réseau cortico-thalamique. L'état actif et l'état silencieux sont tous deux des états stables du réseau, mais les mécanismes de leur alternance sont encore inconnus. Nous montrons, en utilisant des enregistrements intracellulaires multisites chez le chat, que les ondes lentes impliquent tous les neurones néocorticaux et que les périodes actives et les périodes silencieuses débutent en synchronie dans des cellules distantes de jusqu'à 12 mm. L'activité apparaissait principalement à la bordure des aires 5 et 7 et se propageait dans les directions antérieure et postérieure. L'activité débutait plus tôt dans les neurones à décharges rapides (FS) et dans les cellules à décharges par bouffées de potentiels d'action (IB) que dans les autres classes de neurones. Ces résultats procurent une évidence directe pour deux mécanismes de génération de l'état actif : une propagation de l'activité à partir d'un foyer local et une synchronisation d'activité plus faible qui origine de plusieurs endroits. Étonnement, les déclanchements des états silencieux étaient plus précis que les déclanchements des états actifs en ne montrant aucun biais de délai pour un endroit en particulier ou un type de cellule particulier. Cette intrigante découverte démontre le manque de compréhension de la nature des alternances d'états. Nous suggérons que c'est la terminaison synchrone de l'activité et l'occurrence des états silencieux du réseau neuronal qui font l'image de l'EEG pendant le sommeil à ondes lentes si caractéristique. Le déclenchement synchrone du silence dans les neurones distants ne peut reposer sur les propriétés des cellules individuelles et des synapses, comme l'adaptation des décharges neuronales ou la dépression synaptique, mais plutôt, ça implique l'existence d'un mécanisme de réseau. Révéler ce mécanisme à grande échelle encore inconnu, qui change l'activité du réseau au silence, va aider notre compréhension de l'origine des rythmes du cerveau dans ses fonctions normales et pathologiques.

3.2 Abstract

Slow-wave sleep is characterized by alternating periods of activity and silence in cortico-thalamic networks. Both, activity and silence are stable network states, but the mechanisms of their alternation remain unknown. We show, using simultaneous multisite intracellular recordings in cats, that slow rhythm involves all neocortical neurons, and that both, activity and silence started synchronously in cells located up to 12 mm apart. Activity appeared predominantly at area 5/7 border, and spread in both, anterior and posterior directions. The activity started earlier in fast-spiking and intrinsically-bursting cells, than in neurons of other classes. These results provide direct evidence for two mechanisms of active state generation: spread of activity from a local focus, and synchronization of weaker activity, originated at multiple locations. Surprisingly, onsets of silent states were synchronized even more precisely than the onsets of activity, showing no latency bias for location or cell type. This most intriguing finding exposes a major gap in understanding the nature of state alternation. We suggest that it is the synchronous termination of activity and occurrence of silent states of the neuronal network that makes the EEG picture during slow wave sleep so characteristic. Synchronous onset of silence in distant neurons cannot rely on properties of individual cells and synapses, like adaptation of neuronal firing or synaptic depression, instead, it implies the existence of a network mechanism. Revealing this yet unknown large-scale mechanism, which switches network activity to silence, will aid our understanding of the origin of brain rhythms in normal function and pathology.

3.3 Introduction

Slow, large amplitude fluctuations of the cumulative electrical activity of the brain are a hallmark of the periods of slow wave sleep (1). These slow, below 4 Hz, rhythms in the electroencephalogram (EEG) reflect alternating periods of activity and silence in thalamocortical networks (2-7). The active states are associated with neuronal depolarization, firing, and rigorous synaptic activity, while during the silent states the neurons are hyperpolarized and the network is inactive (5, 8-11). The alternation of states is of intracortical origin since active and silent states are self-generated in the isolated cortical preparation (2, 12, 13) but are absent in the thalamus of decorticated animals (14). Both, activity and silence are stable states of the network, but the mechanisms of state alternation remain an enigma. One possibility is the origin of activity in a specific local focus, or group of cells, with sequential lateral propagation (12, 15). The propagation hypothesis predicts a similar pattern of initiation and spread of active states, reflected in systematic onset delays between cortical sites. A necessary requirement for this mechanism to work is that the focal activity must be strong enough to evoke discharges in target cells and thus to expand over the neural network. Alternatively, weaker activity may originate occasionally at multiple locations, and involve further parts of the network if appears synchronously enough (13, 16). The synchronization hypothesis predicts a variable pattern of activity initiation and spread, no systematic delays between sites, and occurrence of occasional local episodes of activity at any site. To trigger a generalized active state by this mechanism, sufficient number of sites must become active within an integration period of postsynaptic responses. These hypotheses suggest an explanation of the origin of active states. Termination of activity and onset of silent states is ascribed to the intrinsic cellular properties and currents (17-20). Since each neuron has a unique set of intrinsic currents, such a mechanism inevitably implies high variability of silent state onsets in individual cells. To test these predictions, we recorded simultaneously local field potentials (LFP) and intracellular activity of 3-4 neurons in cat neocortex. We show that slow rhythm involves all neocortical neurons, and that onsets of both, activity and silence, occurs with high temporal precision in cells located up to 12 mm apart. Our results provide direct evidence for two mechanisms of active state generation: spread of activity from a local focus, and synchronization of

weaker activity, originated at multiple locations. Most surprisingly, onsets of silent states were synchronized even more precisely than the onsets of activity. We suggest that it is the synchronous termination of activity and occurrence of silent states of the neuronal network that makes the EEG picture during slow wave sleep so characteristic.

3.4 Results

We recorded simultaneously the LFP and intracellular activity of 3-4 neurons in cat neocortex (Fig. 1). In membrane potential traces of 4 simultaneously recorded cells (Fig 1b), the active, depolarized states are unambiguously distinguishable from the silent, hyperpolarized states. Two features are immediately apparent in the simultaneously recorded cells. First, all cells are involved in the rhythm of the slow LFP oscillations. Membrane potential traces of all 4 cells showed clear relation to the LFP signal, although occasionally a cell may skip few activity cycles (Fig. 1b, shadowed period). Second, all simultaneously recorded neurons showed very similar pattern of membrane potential changes. In all 4 cells, the alternation between active and silent states was synchronized on a coarse time scale, with common periods of activity or silence.

To compare the timing of the onsets of activity and silence quantitatively, we detected active and silent states in 23 sets of 4 (n=10) or 3 (n=13) simultaneously recorded neurons. In each cell (n=103), the states were detected using two methods. In the first method, we used membrane potential levels as thresholds for state detection (Fig. 2a,b). During active states, cells were depolarized by 9.7±4.95 mV (mean + SD) relative to the silent states, and the membrane potential fluctuated stronger, with the standard deviation (SD), 3.26±1.57 mV during active states vs. 1.04±0.45 mV during silent states (n=103, $p<0.001$). Our second method of state detection exploits this difference. We calculated the mean membrane potential and its SD in a running window of 25 ms, and plotted a 3D distribution of the occurrence of pairs of mean and SD values (Fig. 2c,d). Silent states formed a sharp peak at hyperpolarized potentials and low SD values. Active states are represented in this plot by a broader hill at more depolarized potentials and higher SD values. Since peak location differs along both axes, the use of a combination of these two parameters improves the detection and separation of the states (Fig. 2c,d).

Having detected the onsets of active and silent states, we can now address the question: Were there specific temporal patterns of involvement of neurons from different locations in active or silent states? We used two strategies to investigate this question. First, we searched for possible patterns during generalized states, in which all simultaneously

recorded cells, separated by 4 mm intervals in antero-posterior direction were involved (Fig. 3a). Such groups of active (or silent) states in 4 cells will be referred to as "clusters" (Fig. 3b). For every cluster, we calculated delays of state onset in each cell relative to the cluster mean. If an active state would typically originate in a specific focus and then spread, as the propagation hypothesis predicts, the cell which is closest to that focus would be leading in the clusters and thus have negative delays. Data in Figure 3c for the active state clusters supports this scenario. Cell-2 had a strong tendency to lead (averaged delay -22.5±27.5 ms), while cell-4 had a strong tendency to follow (averaged delay +20.2 ±46.1 ms, $p<0.001$, n=138). In cell-3, located between the neurons 2 and 4, the clustered active states had intermediate delays (average -1.9±49.7 ms). However, the above relation was not absolute, and active state clusters with a "reversed" order, with cell-4 leading and cell-2 following, were occasionally observed (Fig. 3,b4). Furthermore, the dispersion of the delays was high in every cell and all distributions covered zero, implying that any cell could be leading in some clusters (negative delays), while following in others (positive delays). Despite these reservations, the results strongly suggest that active states originated most often at, or close to, the cell-2 location, and then spread in both directions. Population analysis of 23 sets of simultaneously recorded cells further supports this scenario (Fig. 3,d1). In 21 neurons recorded at the border between area 5 and area 7 (position 2), averaged delays of clustered active states were negative (-14.6±12.9 ms, n=21) and significantly different from the positive delays in more posteriorly recorded cells (6.1+14.8 ms, n=17, $p<0.0016$ at position 3 and 11.9 ±8.8 ms, n=23, $p<0.001$ at position 4).

In another approach we analyzed state onset in 104 pairs of simultaneously recorded cells (Fig. 3e). Since more states contribute to a pair-wise comparison, we consider it a useful supplement to the analysis of clusters. The pair-wise analysis confirmed the results obtained for clustered states. Cells, located 8-12 mm more posteriorly, were involved in active states with a delay of 7.8±7.9 ms (8 mm, n=33) and 6.1±7.2 ms (12 mm, n=18) relative to more anteriorly-located reference cells (Fig. 3,e1). At 4 mm distance, the delays were not significantly different from zero (1.4±9.0 ms, n=53), apparently because active states originated not from the most anterior position.

Did active states originate in cells of a specific type? We classified the cells by their intrinsic firing patterns (21) as regular-spiking (RS), fast-rhythmic-bursting (FRB), intrinsic-bursting (IB) and fast-spiking (FS, Fig. 4a). In state clusters, active states appeared first in the FS cells (averaged delay–7.8±14.6 ms, $p=0.015$, $n=21$), followed by IB neurons (delay -5.45±19.57 ms, $p>0.1$, $n=16$) (Fig. 4,b1). Pair-wise comparison confirmed the results of analysis of state clusters. In the pairs consisting of an FS and an RS cell the active states in the FS neurons started earlier, with an average delay of –7.3±11.6 ms ($p=0.0014$, $n=31$ pairs).

In marked contrast to the above results, similar analyses of silent state onsets provided no evidence for preferential origin at specific locus or specific cell type. The averaged delays of clustered silent states in cells 1-4 in Figure 3,a-c were 5.3±31.7 ms; –2.5±23.4 ms; 3.9±40.0 ms; and –6.7±37.2 ms ($p>0.1$ for all pairs). Population analysis of the silent state onsets in 23 sets and 104 pairs of simultaneously recorded neurons did not reveal any significant latency bias for any particular location (Fig. 3,d2) or relative position of recorded cells (Fig. 3,e2; 0.14±11.0 ms at 4 mm distance, 2.3±7.6 ms at 8 mm and 1.9±8.6 ms at 12 mm) or cell type (Fig. 4,b2). For the silent states, the FS neurons had only a non-significant tendency to lead in clusters (–5.6±20.5 ms) and in the FS-RS pairs (–2.9±13.8 ms, $p>0.1$ in both cases).

Comparison between active and silent states revealed the most interesting fact, namely, that silent states begin in simultaneously recorded cells more synchronously than active states. Several lines of evidence corroborate this conclusion. In state clusters, the SD of onset delays was lower for the silent states than for the active states (34.4±11.6 ms vs. 39.7±11.3 ms, $p=0.0011$, $n=103$, Fig. 4d), showing that the silent states started with a higher temporal precision in different cells. This point is further stressed by the absence of significant dependencies of the onset of the silent states on the location (Fig. 3,d2,e2) or cell type (Fig. 4,b2). The proportion of states, which formed clusters in simultaneously recorded neurons was higher for the silent than for the active states (50.6±19.0% vs. 45.1±17.3%, $p=0.0021$, $n=103$, Fig. 4c). The higher percent of clustered states implies that the cases when all simultaneously recorded cells entered the silent state were encountered more often than those cases when all cells became active together. Finally, the pair-wise

analysis also revealed lower SD of silent states onset than of the active states (30.1±8.7 ms vs. 33.8±8.6 ms, $p<0.001$, n=121 pairs).

3.5 Discussion

We found direct evidence for both suggested mechanisms of active state generation: spread of activity from a local focus (12, 15), and synchronization of weaker activity, originated at multiple locations (13, 16). The focal origin and spread hypothesis is supported by the finding that active states appear predominantly at the border between areas 5 and 7, and spread from there in both directions. Together with recent analysis of high-density EEG in humans (16), our data suggests the presence of cortical regions with enhanced intrinsic excitability, which could primarily generate active states during sleep oscillations. Earlier onset of activity in FS and IB cells than in other neurons shows, that a specific cell type may underlie the origin of active states in cat neocortex (12). Two observations cannot be explained by activity spread from a local focus, but lend support to the hypothesis on multiple sources and synchronization of activity. At any recording site we have observed local activity episodes, not accompanied by activity in the other simultaneously recorded neurons. Moreover, "typical" sequences of involvement of cells in generalized active states occurred in line with alternative sequences, including "reversed" order. One important implication of the direct evidence for two mechanisms of active state generation is that the necessary requirements for both are fulfilled. Hence during slow-wave sleep, thalamocortical networks can support both, spread of activity from a local focus (12, 15), as well as synchronization of activity originating from different loci (13, 16). It is tempting to speculate, that the efficacy of these mechanisms may increase in pathology, eventually leading to seizures.

Our most intriguing finding is the high synchrony of the silent state onsets. It exposes a major gap in understanding the nature of state alternation. We suggest that it is the synchronous termination of activity and occurrence of silent states of the neuronal network, which produces the characteristic EEG pattern of the slow wave sleep. Our results allow to

exclude several candidate mechanisms of activity termination. Active and silent states are not due to alternating activity of two mutually inhibiting neuronal sub-populations, because all cells were involved in the slow rhythm, and we never observed a cell to be systematically active while other neurons were silent. Unlike for active states, we find no evidence for preferential onset of silent states at any specific location, thus excluding the possibility of a local focus and spread of silence in a kind of spreading depression. Intrinsic membrane properties of neurons or synaptic depression can be also excluded as major causes for synchronous activity termination, since both are extremely non-uniform in different cells and synapses (22, 23). Instead, the high synchrony of the silent state onsets implies the existence of a network mechanism which switches activity to silence. One possibility is synchronization among inhibitory cells, which eventually discharge synchronously enough to silence the whole network. Fast spiking and low-threshold spiking cortical interneurons are electrotonically coupled (24, 25). During slow-wave oscillation, neuronal activity leads to a decrease of extracellular calcium concentration (26), thus facilitating electrotonical coupling of neurons and glial cells (27). Finally, cortical activity can recruit intrinsic oscillatory mechanisms in thalamocortical neurons (28), which could increase synchrony among inhibitory interneurons. Indeed, synchrony in the silent state onset is disrupted in neocortical slabs (13). The above hypothesis predicts an increase of synchrony of membrane potential fluctuations in inhibitory interneurons towards the end of an active state. This should lead to the higher incidence of strong IPSPs in neocortical cells. Further, if inhibitory neurons exert a synchronizing effect on activity in the neocortex, as they do in the hippocampus (29), synchrony of the membrane potential fluctuations in all cells might also increase. Experimental testing of these predictions is technically an extremely challenging task, but it will lead to further insights into the mechanisms of slow-wave sleep and the origin of brain rhythms.

3.6 Materials and Methods

3.6.1 Surgery and recording

All experimental procedures used in this study were performed in accordance with the Canadian guidelines for animal care and were approved by the committee for animal care of Laval University.

Experiments were conducted on adult cats under a mixture of ketamine-xylazine and thiopental anesthesia (10-15 mg/kg ketamine, 2-3 mg/kg xylazine and 10 mg/kg thiopental). We opted for this type of anesthesia because it reproduces closely typical for the natural sleep EEG patterns, including the slow-wave oscillations. Details of the experimental procedures are described elsewhere (30, 31) and in the online supporting material. Briefly, surgery was started after the EEG showed typical signs of general anesthesia and complete analgesia was achieved. Additional doses of anesthetics were administrated when the EEG showed changes towards activated patterns. Craniotomy was made at coordinates AP –5 to +18, L 3 to 12, to expose the suprasylvian gyrus. Four electrodes for intracellular recording were positioned in neocortical areas 5, 7 and 21, along the suprasylvian gyrus at 4 mm intervals. The electrode for the LFP recording was located between positions of intracellular electrodes 2 and 3. After positioning of the electrodes, the craniotomy was filled with 3.5-4% agar (Sigma). With each intracellular electrode, several cells were sequentially recorded and stained in one experiment. The LFP and intracellular activity of 3-4 neurons were recorded simultaneously.

3.6.2 Morphological procedures

After experiments the animals were perfused, with 0.9% saline, followed by 3% paraformaldehyde, the brain around recorded sites was placed in 30% sucrose, sectioned

and then processed by standard procedures (32). Reconstruction of stained cells was done with a computerized Neurolucida system.

3.6.3 Data processing

Offline data processing was done with custom-written programs in MatLab (Mathworks Inc) environment.

3.6.3.1 Clusters of states

We defined as "clusters" groups of states, which fulfill two criteria. First, they should occur in all simultaneously recorded cells. Second, their onsets should be separated by less than 200 ms. Thus, number of states in one cluster is equal to the number of simultaneously recorded cells. Within each cluster we calculated delays of the onsets of states in each cell relative to the cluster mean. After completing these calculations, we had: (i) for a set of simultaneously recorded cells, number of clusters; (ii) for each cell, delays of state onsets in that cell relative to the cluster mean, and (iii) for each cell, we calculated portion of the states contributed to clusters out of the total number of states in this cell.

3.6.3.2 Statistical analysis

For statistical analysis we used subroutines of MatLab Statistics Toolbox and SPSS for Windows (SPSS Inc.). Throughout the text, mean values are given together with SD (mean + SD).

3.7 Acknowledgements

We are grateful to Marina Chistiakova for comments and discussions and Dimitrios Giannikopoulos for improving the English. We thank Pierre Giguere for technical assistance. This work was supported by grants from CIHR and NSERC of Canada (to IT) and DGF to MV. IT is CIHR scholar.

3.8 References

1. Blake, H. & Gerard, R. W. (1937) Am J Physiol 119, 692-703.
2. Steriade, M., Nuñez, A. & Amzica, F. (1993) J Neurosci 13, 3252-3265.
3. Steriade, M., Nuñez, A. & Amzica, F. (1993) J Neurosci 13, 3266-3283.
4. Steriade, M., Timofeev, I. & Grenier, F. (2001) J Neurophysiol 85, 1969-85.
5. Timofeev, I., Grenier, F. & Steriade, M. (2001) Proc Natl Acad Sci U S A 98, 1924-1929.
6. Petersen, C. C. H., Hahn, T. T. G., Mehta, M., Grinvald, A. & Sakmann, B. (2003) Proc Natl Acad Sci U S A 100, 13638-13643.
7. Contreras, D. & Steriade, M. (1995) J Neurosci 15, 604-22.
8. Wilson, C. J. & Kawaguchi, Y. (1996) J Neurosci 16, 2397-2410.
9. Timofeev, I., Contreras, D. & Steriade, M. (1996) J Physiol 494, 265-78.
10. Shu, Y., Hasenstaub, A. & McCormick, D. A. (2003) Nature 423, 288-93.
11. Contreras, D., Timofeev, I. & Steriade, M. (1996) J Physiol 494, 251-64.
12. Sanchez-Vives, M. V. & McCormick, D. A. (2000) Nat Neurosci 3, 1027-34.
13. Timofeev, I., Grenier, F., Bazhenov, M., Sejnowski, T. J. & Steriade, M. (2000) Cereb Cortex 10, 1185-1199.
14. Timofeev, I. & Steriade, M. (1996) J Neurophysiol 76, 4152-68.
15. Cossart, R., Aronov, D. & Yuste, R. (2003) Nature 423, 283-8.
16. Massimini, M., Huber, R., Ferrarelli, F., Hill, S. & Tononi, G. (2004) J Neurosci 24, 6862-6870.
17. Bazhenov, M., Timofeev, I., Steriade, M. & Sejnowski, T. J. (2002) J Neurosci 22, 8691-704.
18. Compte, A., Sanchez-Vives, M. V., McCormick, D. A. & Wang, X.-J. (2003) J Neurophysiol 89, 2707-2725.
19. Hill, S. L. & Tononi, G. (2004) J Neurophysiol 93, 1671-1698.
20. Milojkovic, B. A., Radojicic, M. S. & Antic, S. D. (2005) J Neurosci 25, 3940-51.
21. Steriade, M. (2004) Nat Rev Neurosci 5, 121-34.
22. Markram, H., Toledo-Rodriguez, M., Wang, Y., Gupta, A., Silberberg, G. & Wu, C. (2004) Nat Rev Neurosci 5, 793-807.
23. Thomson, A. M. & Deuchars, J. (1994) Trends Neurosci 17, 119-26.
24. Galarreta, M. & Hestrin, S. (1999) Nature 402, 72-5.
25. Gibson, J. R., Beierlein, M. & Connors, B. W. (1999) Nature 402, 75-9.
26. Massimini, M. & Amzica, F. (2001) J Neurophysiol 85, 1346-50.
27. Thimm, J., Mechler, A., Lin, H., Rhee, S. & Lal, R. (2005) J Biol Chem 280, 10646-10654.
28. Hughes, S. W., Cope, D. W., Blethyn, K. L. & Crunelli, V. (2002) Neuron 33, 947-58.
29. Cobb, S. R., Buhl, E. H., Halasy, K., Paulsen, O. & Somogyi, P. (1995) Nature 378, 75-8.
30. Crochet, S., Chauvette, S., Boucetta, S. & Timofeev, I. (2005) Eur J Neurosci 21, 1030-1044.
31. Rosanova, M. & Timofeev, I. (2005) J Physiol 562.2, 569-582.
32. Horikawa, K. & Armstrong, W. E. (1988) J Neurosci Methods 25, 1-11.

3.9 Figure legends

Figure 1. Active and silent states in 4 simultaneously recorded neurons and in the EEG. a, Location and morphology of cells recorded in one experiment. Four electrodes for intracellular recordings were positioned at 4 mm intervals along the suprasylvian gyrus, in areas 5, 7 and 21 (inset). With each intracellular electrode, several cells were sequentially recorded and stained. An overview shows in different colors reconstructions of all cells from this experiment. a1-a4, expanded view of 4 simultaneously recorded neurons. Cells a1 and a3 were pyramids. Cells a2 and a4 had non-pyramidal morphology, but were also excitatory, as judged by their spiny dendrites (not shown). b, Simultaneously recorded EEG and membrane potential of 4 cells, shown in a1-a4. The EEG electrode was positioned between the intracellular recording sites 2 and 3. Membrane potential traces are color coded as in a1-a4. The shadowed area shows a period of silence in cell 1, while the other cells were active.

Figure 2. Two methods of state detection. The first method (a,b) uses membrane potential levels, while the second method (c,d) exploits, in addition to the levels, also the variability of the membrane potential to discriminate between active and silent states. a, Membrane potential trace of a neocortical cell, and expanded view of its part (a1), with threshold levels for state detection and detected states (active: green, silent: red). "States" were defined as periods during which the membrane potential remained above the threshold for active states, or below the threshold for silent states, for >40 ms. To avoid disturbances by transient membrane potential peaks, shorter level crossings were not considered as states (arrows 1, 4), and two active or two silent states separated by <40 ms were extended to fill the gap and pasted together (arrows 2, 3). The levels for state detection were set at equal distances between the peaks of bimodal distribution of the membrane potential values (b). c, 3D density distribution of the data from a. The mean membrane potential and its standard deviation (SD) were calculated in a running window of 25 ms. These values were used as X and Y coordinates; the Z axis is the frequency of their occurrence. d, Top view

of the plot from c, with the regions used for detection of active (green) and silent (red) states outlined. Z axis is grey level-coded.

Figure 3. Clusters of active and silent states in simultaneously recorded cells. a, Membrane potential traces of 4 simultaneously recorded cells and expanded view of its part (b), with state detection levels and detected states (silent: red, active: green). States formed a cluster, if they occurred in all recorded cells with the onsets separated by <200 ms. b1-b5 show examples of "clusters", with clustered states (silent: b1, b3, b5; active: b2, b4) colored, non-clustered states are grey. Vertical interrupted lines: onset of the first state in each cluster. c1, c2, In top panels, each cluster is represented by a blue line, connecting state onsets in all cells. Red line: averaged delays of clustered states in 4 cells. Distance between recorded cells in antero-posterior direction is indicated relative to the most anterior cell. For each cell, distributions of the onsets of clustered states and the portion of clustered states (filled part of the bars) are shown. d1,d2, Mean delay of clustered states plotted against the antero-posterior position of recorded cells. Data for 103 cells (blue symbols) and averages for 4 recording positions (pink: mean and SD). e1, e2, Mean delay of state onsets in simultaneously recorded cell pairs (n=104) plotted against the antero-posterior distance between the cells. Mean delay of state onsets in a more posteriorly located cell was calculated relative to the state onsets in more anteriorly located cell. Other conventions as in (d).

Figure 4. Population analysis of the onsets of active and silent states in simultaneously recorded neurons. a, Electrophysiological identification of neurons. Responses of regular-spiking (RS), fast-rhythmic-bursting (FRB), intrinsically-bursting (IB) and fast-spiking (FS) cells to depolarizing current pulses. b, Relative delays of involvement of cells with different intrinsic membrane properties in clusters of active (b1) and silent (b2) states. Each diamond symbol represents data for one cell; pink symbols are averages for cells of each class (circles: mean, squares: SD). c-d, Comparison of the statistics of clustered active and silent states. Each point represents data for one cell, with the value for the silent states (ordinate) plotted against the respective value for active states (abscissa). c, Number of states involved in clusters, in percent of the total number of states in a cell. d, SD of the onsets of clustered states in a cell.

3.10 Figures

Figure III- 1

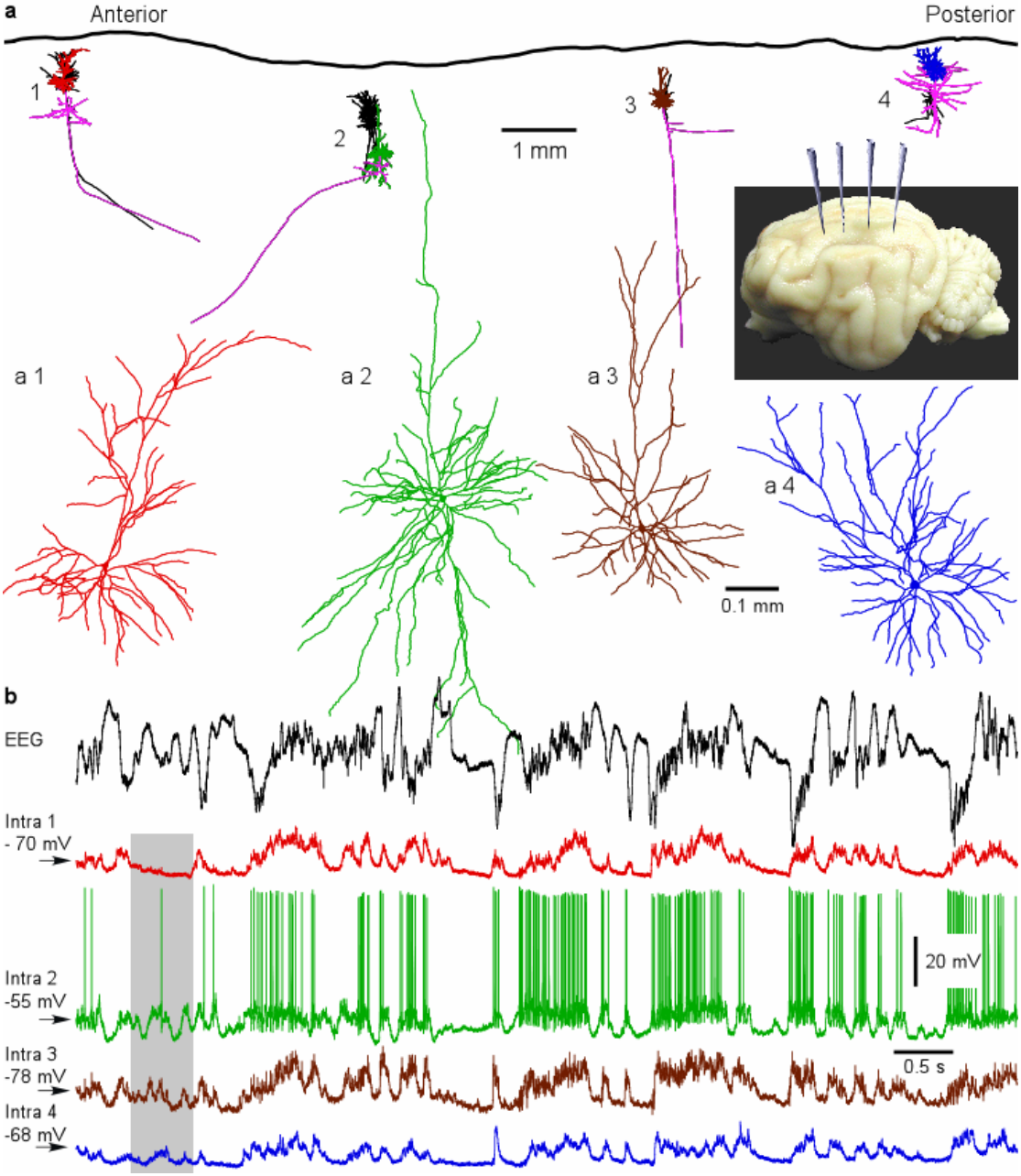

Figure 1.

Figure III- 2

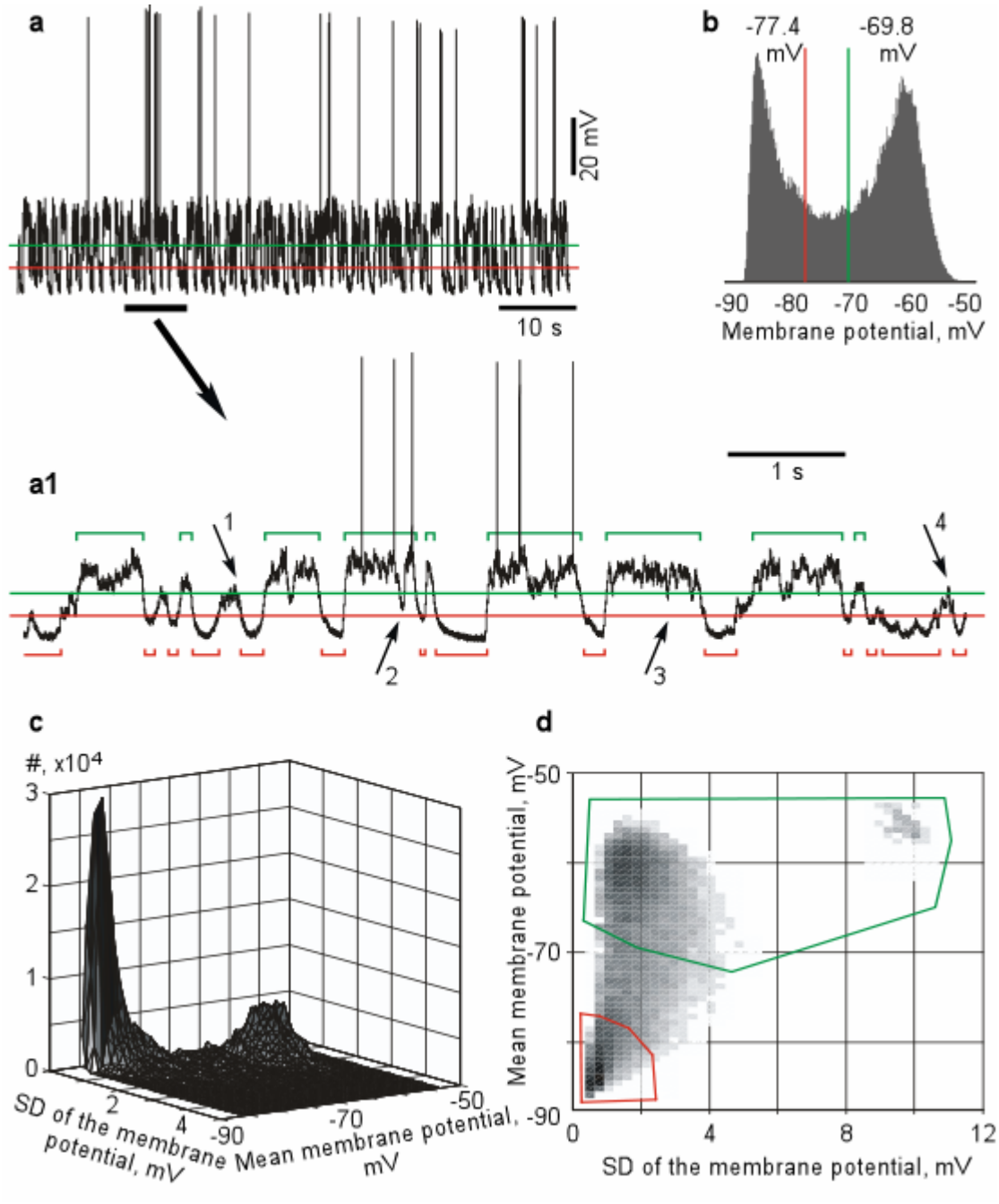

Figure 2.

Figure III- 3 .

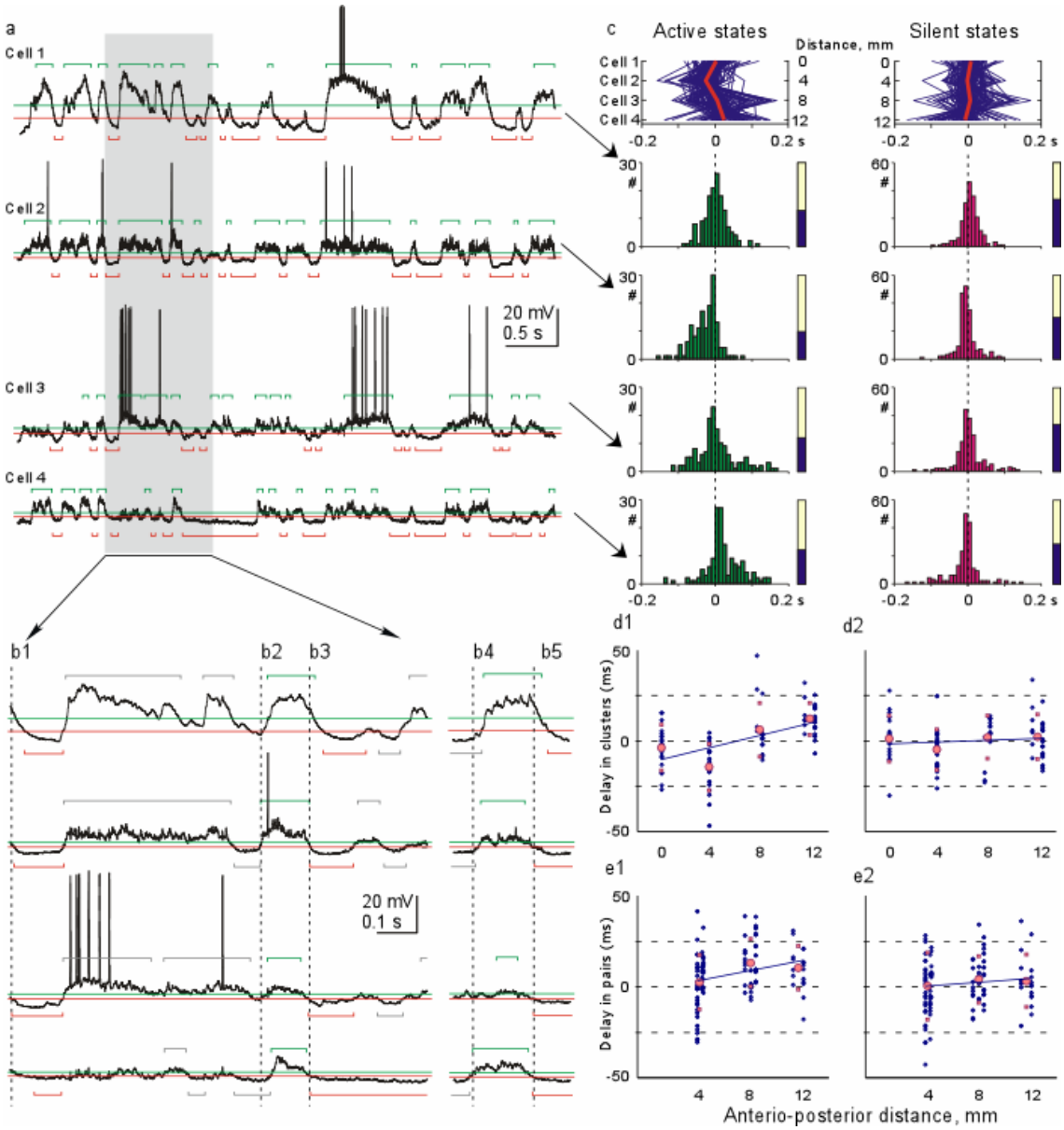

Figure 3.

Figure III- 4

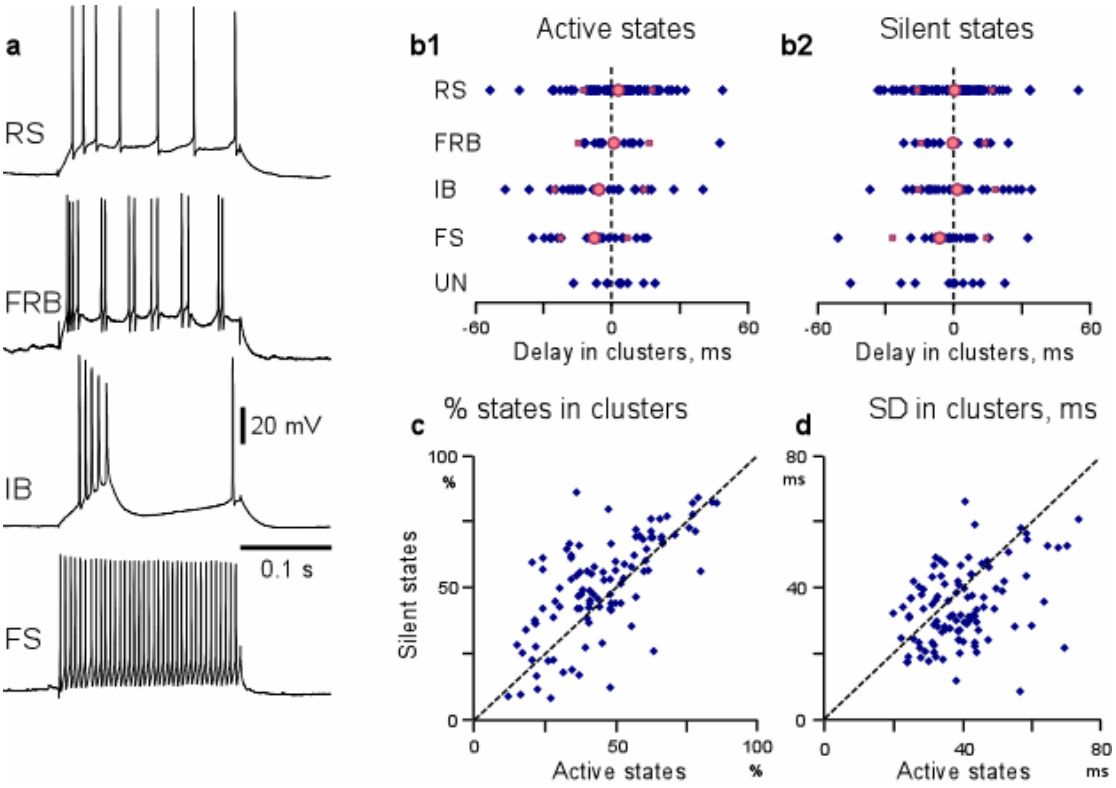

Figure 4.

3.11 Online Supplementary Material

for the manuscript:

Precise long-range synchronization of activity and silence in neocortical neurons

Sylvain Chauvette, Maxim Volgushev, Mikhail Mukovski, Igor Timofeev

3.11.1 Methods

3.11.1.1 Surgery and recording

All experimental procedures used in this study were performed in accordance with the Canadian guidelines for animal care and were approved by the committee for animal care of Laval University.

Experiments were conducted on adult cats under a mixture of ketamine-xylazine and thiopental anesthesia (10-15 mg/kg ketamine, 2-3 mg/kg xylazine and 10 mg/kg thiopental). We opted for this type of anesthesia because it reproduces most closely the electroencephalogram (EEG) patterns typical for natural sleep. Specifically, under this anesthesia both the slow-wave oscillations, spindles and beta-gamma activities are reliably observed in the EEG. Details of the experimental procedures are described elsewhere (1, 2). Briefly, surgery was started after the EEG showed typical signs of general anesthesia and complete analgesia was achieved. Craniotomy was made at coordinates AP –5 to +18, L 3 to 12, to expose the suprasylvian gyrus. The animals were paralyzed with gallamine triethiodide, and artificially ventilated. End-tidal CO2 was held at 3.5-3.7% and body temperature at 37°-38°C. Additional doses of anesthetics were administrated when the EEG showed changes towards activated patterns. To reduce brain pulsations and improve stability of intracellular recording we made bilateral pneumothorax, hip suspension, and

drainage of the cisterna magna. Simultaneous recordings of the local field potential (LFP) and intracellular activity of 3-4 neurons were performed.

Intracellular recordings were made with sharp electrodes, filled with 2.5 M potassium acetate and 2% neurobiotine and beveled to a resistance of 55-80 MOhm. Four electrodes for intracellular recording were positioned in neocortical areas 5, 7 and 21, along the suprasylvian gyrus at 4 mm intervals. Anterio-posterior coordinates of the intracellular electrodes were as following:

Electrode 1: +12, area 5;

Electrode 2: +8, border between area 5 and area 7;

Electrode 3: +4, area 7;

Electrode 4: 0, border between area 7 and area 21.

Lateral coordinates of all intracellular electrodes were between 8 and 9.

LFP's were recorded with coaxial bipolar tungsten electrodes (SNE-100, Rhode Medical Instruments, Summerland, USA). The outer pole of the electrode was positioned on cortical surface and the inner pole was at the depth of 1 mm. The electrode for the LFP recording was located between positions of intracellular electrodes 2 and 3, at coordinates anterior +6, lateral between 7 and 8.

After positioning of the electrodes, the craniotomy was filled with 3.5-4% agar (Sigma). With each intracellular electrode, several cells were sequentially recorded and stained in one experiment.

Intracellular signals were amplified with Neurodata IR-283 amplifiers (Cygnus Technology, PA, USA). The LFP signals were filtered with two band-pass filters, one cutting the frequencies below 0.1 and above 10 kHz, and the other one cutting the frequencies around 60 Hz to reduce the mains-noise. The LFP signal was amplified with the total gain of 1000. Both intracellular and LFP signals were digitized at 20 kHz and recorded on a Vision data acquisition system (Nicolet, WI, USA).

3.11.1.2 Morphological procedures

After experiments the animals were perfused, with 0.9% saline, followed by 3% paraformaldehyde, the brain around recorded sites was placed in 30% sucrose, sectioned and then processed by standard procedures (3). Reconstruction of stained cells was done with a computerized Neurolucida system.

3.11.1.3 Data processing

Offline data processing was done with custom-written programs in MatLab (Mathworks Inc) environment.

3.11.1.4 Detection of active and silent states in membrane potential traces

We detected and separated active and silent states in the membrane potential traces with the use of two approaches.

The first approach was based on clear bimodality of the membrane potential distributions during slow wave oscillations. We set two levels in the bimodal distribution of membrane potential values, which divided the interval between the peaks in three equal parts. The upper level was used as a threshold for detection of active states, and the lower level for detection of the silent states. “States” were defined as periods during which the membrane potential remained above the threshold for active states, or below the threshold for silent states. To avoid disturbances by transient membrane potential peaks, level

crossings for periods shorter than 40 ms were not considered as states. Further, if two active or two silent states were separated by less than 40 ms, the two states were extended to fill the gap and pasted together.

During active states, (i) cells were more depolarized, by 9.7 ± 4.95 mV (mean + SD), than during silent states, and (ii) fluctuations of the membrane potential were significantly higher during active states (SD of the membrane potential 3.26±1.57 mV) than during silent states (SD of the membrane potential 1.04 ± 0.45 mV, $p<0.001$, n=103).

The second approach to state detection exploited two parameters; by which active and silent state differ: (i) membrane potential value and (ii) variability of the membrane potential. We calculated the mean membrane potential and its SD in a running window of 25 ms, and plotted a 3D distribution of the occurrence of pairs of mean and SD values. In this 3D plot, silent states formed a sharp peak at hyperpolarized potentials and low SD values. Active states are represented in this plot by a broader hill at more depolarized potentials and higher SD values. Two regions, one containing the sharp peak representing silent states, and another one containing the peak which represents active states, were delimited on the top view of this plot. Those periods, which were represented by data points within these regions, we classified as respective, active or silent, states. Since location of the two peaks differs along both axes, the use of the combination of these two parameters improves detection and separation of active and silent states. For example, occasional periods of strong inhibition during active state of the network may hyperpolarize a cell below the membrane potential threshold of active state. But since the network remains active, fluctuations of the membrane potential during such period would be still strong, and this period will be correctly assigned to active state. After this initial separation of active and silent states, the procedures against disturbances by occasional membrane potential

peaks were applied: periods shorter than 40 ms were not considered as states, and two active or two silent states separated by less than 40 ms were extended to fill the gap and pasted together.

We detected silent and active states in 103 cells. Averaged duration of active states in these cells was 289±148 ms; average duration of silent state was 201±72 ms.

3.11.1.5 Clusters of states

We defined as "*clusters*" groups of states, which fulfill two criteria. First, they should occur in all simultaneously recorded cells. Second, their onsets should be separated by less than 200 ms. Thus, number of states in one cluster is equal to the number of simultaneously recorded cells. When searching for clusters, states in one cell were taken as reference, and all other simultaneously recorded cells were searched for the states with onsets within 200 ms from onset of states in the reference cell. During this search, only closest possible neighbors were considered. For example, if a cell had two states of 80 ms length, with the onsets of both of them occurring with less than 200 ms difference from the onset of a state in the reference cell (say, -60 and +140 ms), only the state with the onset closest to the onset of the state in reference cell was considered for a cluster (in this case, the state with –60 ms delay). After detecting clusters of states, we calculated within each cluster delays of the onsets of states in each cell relative to the cluster mean. After completing these calculations, we had: (i) for a set of simultaneously recorded cells, number of clusters; (ii) for each cell, delays of state onsets in that cell relative to the cluster mean, and (iii) for each cell, we calculated portion of the states contributed to clusters out of the total number of states in this cell.

3.11.1.6 Electrophysiological types of cells

A simplistic classification of cells into 4 electrophysiological classes (4) with differential intrinsic membrane properties: regular-spiking (RS), fast-rhythmic-bursting (FRB), intrinsically-bursting (IB) and fast-spiking (FS) was made on the basis of responses of the cells to depolarizing current pulses. As additional criteria, shape of action potentials, generated in response to current application and without stimulation and firing pattern without stimulation was taken into account. For example, during both, current evoked activity and occasionally without stimulation, FS neurons generated very short action potentials, FRB cells generated characteristic duplets or triplets of action potentials, and IB cells produced typical bursts.

3.11.1.7 Statistical analysis

For statistical analysis we used subroutines of MatLab Statistics Toolbox and SPSS for Windows (SPSS Inc.). Throughout the text, mean values are given together with SD (mean $\pm$ SD).

3.11.2 References

1. S. Crochet, S. Chauvette, S. Boucetta, I. Timofeev, *Eur J Neurosci* **21**, 1030-1044 (2005).
2. M. Rosanova, I. Timofeev, *J Physiol* **562.2**, 569-582 (2005).
3. K. Horikawa, W. E. Armstrong, *J Neurosci Methods* **25**, 1-11 (1988).
4. M. Steriade, *Nat Rev Neurosci* **5**, 121-34 (Feb, 2004).

Chapter IV

4. General Conclusion

Sleep is an ubiquitous phenomenon in the animal kingdom; it has been find in mammals, birds, invertebrates, and recently, sleep has been described in drosophila (Shaw et al., 2000). Both the physiological role of sleep for the brain and most of the mechanisms underlying the generation of sleep rhythms are hotly debated (Timofeev and Bazhenov, 2005). Here, we investigated the mechanism of generation of the slow oscillation that is the major rhythm occurring during slow-wave sleep. To address this question, we used different methods, namely 16 simultaneous LFP recordings from superficial to deep cortical layer in anesthetized and naturally sleeping cats, up to four simultaneous intracellular recordings of closely located cells (< 200 μm) or distantly located cells (up to 12 mm) from anesthetized cats, and simultaneous closely located dual intracellular recordings from naturally sleeping cats. It is well known that slow oscillations are well synchronized in cortical neurons during slow-wave sleep, but this is true only on coarse time scale. When we analyzed our data at fine time scale, we observed that closely located as well as distantly located cells could be activated with delays of up to few tens of millisecond. Such high variability suggests local origin of slow EEG waves.

It was shown that slow wave activity is enhanced locally by learning task (Huber et al., 2004) which reinforces the hypothesis of a local mechanism. In the work of Huber and colleagues, it was shown that learning task involving specific brain regions (in that case, a rotating task involving Brodmann areas 40 and 7) produced a rebound increase of slow wave activity in these areas during the following sleep. They also showed that the local increase in slow wave activity after learning correlates with improved performance of the task after sleep, suggesting that sleep is important for memory consolidation as suggested in the review of Steriade and Timofeev (Steriade and Timofeev, 2003). Multiples studies have associated slow-wave sleep with memory consolidation of a learned task (Gais et al., 2000; Stickgold et al., 2000a; Stickgold et al., 2000b; Maquet, 2001; Huber et al., 2004).

The active state of the slow oscillation is associated with a decrease of extracellular calcium in neocortex (Massimini and Amzica, 2001; Crochet et al., 2005) and also the

spindles are associated with rhythmic and synchronous spike burst of thalamic neurons, which depolarizes the dendrites of neocortical neurons and which, in turn, is associated with a massive Ca^{2+} entry (Yuste and Tank, 1996). As hypothesized in modeling studies (Destexhe and Sejnowski, 2001), this may provide an effective signal to efficiently activate Ca^{2+} calmodulin-dependent protein kinase II (CaMKII) that is implicated in synaptic plasticity of excitatory synapses in cortex and other site in the nervous system (Soderling and Derkach, 2000). Thus, the slow oscillations could provide the long timescales needed to mobilize the machinery responsible for the consolidation of memory traces acquired during state of wakefulness (Steriade and Timofeev, 2003).

Slow oscillations are believed to originate from neocortex, because slow oscillation could be obtained from athalamic animals (Steriade et al., 1993b) and other isolated cortical preparations (Sanchez-Vives and McCormick, 2000; Timofeev et al., 2000b), but absent in the thalamus of decorticated animals (Timofeev and Steriade, 1996). We showed that active state could originate in any layer of the neocortex but with tendency to originate in deep layers. In addition, IB cells from any layer have tendency to be first activated. The hypothesis of summation of independent-mediator released proposed in 2000 (Timofeev et al., 2000b) is still valid and could explain the tendency of deep layer V pyramidal cells to be activated first. In fact, layer V pyramidal cells have a large soma with large spiny apical dendrite that reaches layer I, thus receiving thousand of inputs. These cells are more likely to receive depolarizing potentials from independently released mediators. In addition, the burst firing mode of these neurons is likely more effective in depolarizing postsynaptic cells up to firing threshold (Lisman, 1997) and initiate the active state.

The surprising fact that silent states are much more synchronously initiated suggests a network mechanism. It is already known that silent states are associated with periods of disfacilitation (Timofeev et al., 2001a) that are dominated by potassium currents. The onset of silent state could arise from a synchronous firing of inhibitory cells. It is known that extracellular calcium concentration decrease with time during active state (Massimini and Amzica, 2001; Crochet et al., 2005) and that interneurons are coupled via gap junctions (Galarreta and Hestrin, 1999; Gibson et al., 1999; Galarreta and Hestrin, 2001). It was also

shown that gap junctions are more effective when extracellular calcium concentration is low (Thimm et al., 2005), which could increase interneuronal electrical coupling. Thus, either large scale network synchronizing mechanism or interneuronal electrical coupling or both are responsible for the synchronous termination of active states.

Futures studies should be done with non-anesthetized animals to make sure that no bias is induced by the anesthetic. Also, very little is known about the initiation of silent state. We found that silent state were initiated much more synchronously that active state, but no studies have describe the mechanism of silent state initiation. One of the ways study the mechanism of silent states initiation is to use specific potassium channel antagonists to affect the generation of theses silent states and to determine if one type or many types of channels are responsible for the generation of silent state. Knowing which channel(s) is/are affecting the generation of silent state would allow us to determine a clear mechanism of silent state generation. Another approach is to perform multisite intracellular recordings from closely located neurons followed by morphological and histochemical identification of the leading neurons.

Bibliography

Achermann P, Borbely AA (1997) Low-frequency (< 1 Hz) oscillations in the human sleep electroencephalogram. Neuroscience 81:213-222.

Amzica F, Steriade M (2002) The functional significance of K-complexes. Sleep Med Rev 6:139-149.

Anderson JC, Douglas RJ, Martin KA, Nelson JC (1994) Map of the synapses formed with the dendrites of spiny stellate neurons of cat visual cortex. J Comp Neurol 341:25-38.

Aserinsky E, Kleitman N (1955) Two types of ocular motility occurring in sleep. J Appl Physiol 8:1-10.

Bal T, McCormick DA (1993) Mechanisms of oscillatory activity in guinea-pig nucleus reticularis thalami in vitro: a mammalian pacemaker. J Physiol 468:669-691.

Bal T, McCormick DA (1996) What stops synchronized thalamocortical oscillations? Neuron 17:297-308.

Bannister NJ, Nelson JC, Jack JJ (2002) Excitatory inputs to spiny cells in layers 4 and 6 of cat striate cortex. Philos Trans R Soc Lond B Biol Sci 357:1793-1808.

Bazhenov M, Timofeev I, Steriade M, Sejnowski TJ (1999) Self-sustained rhythmic activity in the thalamic reticular nucleus mediated by depolarizing GABAA receptor potentials. Nat Neurosci 2:168-174.

Bazhenov M, Timofeev I, Steriade M, Sejnowski TJ (2002) Model of thalamocortical slow-wave sleep oscillations and transitions to activated States. J Neurosci 22:8691-8704.

Benington JH, Woudenberg MC, Heller HC (1995) Apamin, a selective SK potassium channel blocker, suppresses REM sleep without a compensatory rebound. Brain Res 692:86-92.

Blake H, Gerard RW (1937) Brain potentials during sleep. Am J Physiol 119:692-703.

Borg-Graham LJ, Monier C, Fregnac Y (1998) Visual input evokes transient and strong shunting inhibition in visual cortical neurons. Nature 393:369-373.

Boucetta S, Crochet S, Chauvette S, Timofeev I (Submitted 2005) Extracelleular Ca 2+ fluctuations during slow oscillation affect AHP and modify firing properties of neocortical neurons. J Physiol.

Bouyer JJ, Montaron MF, Rougeul A (1981) Fast fronto-parietal rhythms during combined focused attentive behaviour and immobility in cat: cortical and thalamic localizations. Electroencephalogr Clin Neurophysiol 51:244-252.

Bressler SL (1990) The gamma wave: a cortical information carrier? Trends Neurosci 13:161-162.

Brumberg JC, Nowak LG, McCormick DA (2000) Ionic mechanisms underlying repetitive high-frequency burst firing in supragranular cortical neurons. J Neurosci 20:4829-4843.

Budde T, Biella G, Munsch T, Pape HC (1997) Lack of regulation by intracellular Ca2+ of the hyperpolarization-activated cation current in rat thalamic neurones. J Physiol 503 (Pt 1):79-85.

Buhl EH, Tamas G, Szilagyi T, Stricker C, Paulsen O, Somogyi P (1997) Effect, number and location of synapses made by single pyramidal cells onto aspiny interneurones of cat visual cortex. J Physiol 500 (Pt 3):689-713.

Burkhalter A (1989) Intrinsic connections of rat primary visual cortex: laminar organization of axonal projections. J Comp Neurol 279:171-186.
Buxhoeveden DP, Casanova MF (2002a) The minicolumn and evolution of the brain. Brain Behav Evol 60:125-151.
Buxhoeveden DP, Casanova MF (2002b) The minicolumn hypothesis in neuroscience. Brain 125:935-951.
Callaway EM (2002) Cell type specificity of local cortical connections. J Neurocytol 31:231-237.
Cardin JA, Palmer LA, Contreras D (2005) Stimulus-dependent gamma (30-50 Hz) oscillations in simple and complex fast rhythmic bursting cells in primary visual cortex. J Neurosci 25:5339-5350.
Chagnac-Amitai Y, Luhmann HJ, Prince DA (1990) Burst generating and regular spiking layer 5 pyramidal neurons of rat neocortex have different morphological features. J Comp Neurol 296:598-613.
Cipolloni PB, Peters A (1983) The termination of callosal fibres in the auditory cortex of the rat. A combined Golgi--electron microscope and degeneration study. J Neurocytol 12:713-726.
Cirelli C, Bushey D, Hill S, Huber R, Kreber R, Ganetzky B, Tononi G (2005) Reduced sleep in Drosophila Shaker mutants. Nature 434:1087-1092.
Cisse Y, Grenier F, Timofeev I, Steriade M (2003) Electrophysiological properties and input-output organization of callosal neurons in cat association cortex. J Neurophysiol 89:1402-1413.
Colonnier M (1981) The electron-microscopic analysis of the neuronal organization of the cerebral cortex. In: The organization of the cerebral cortex (Schmitt F. O, Worden F. G, Dennis S. G, eds), pp 125-152. Cambridge: MIT press.
Connors BW, Gutnick MJ (1990) Intrinsic firing patterns of diverse neocortical neurons. Trends Neurosci 13:99-104.
Contreras D, Steriade M (1995) Cellular basis of EEG slow rhythms: a study of dynamic corticothalamic relationships. J Neurosci 15:604-622.
Contreras D, Curro Dossi R, Steriade M (1992) Bursting and tonic discharges in two classes of reticular thalamic neurons. J Neurophysiol 68:973-977.
Contreras D, Curro Dossi R, Steriade M (1993) Electrophysiological properties of cat reticular thalamic neurones in vivo. J Physiol 470:273-294.
Contreras D, Timofeev I, Steriade M (1996) Mechanisms of long-lasting hyperpolarizations underlying slow sleep oscillations in cat corticothalamic networks. J Physiol 494 (Pt 1):251-264.
Cossart R, Aronov D, Yuste R (2003) Attractor dynamics of network UP states in the neocortex. Nature 423:283-288.
Cragg BG (1967) The density of synapses and neurones in the motor and visual areas of the cerebral cortex. J Anat 101:639-654.
Crochet S, Chauvette S, Boucetta S, Timofeev I (2005) Modulation of synaptic transmission in neocortex by network activities. Eur J Neurosci 21:1030-1044.
DeFelipe J, Farinas I (1992) The pyramidal neuron of the cerebral cortex: morphological and chemical characteristics of the synaptic inputs. Prog Neurobiol 39:563-607.
DeFelipe J, Hendry SH, Jones EG (1986) A correlative electron microscopic study of basket cells and large GABAergic neurons in the monkey sensory-motor cortex. Neuroscience 17:991-1009.

DeFelipe J, Hendry SH, Hashikawa T, Molinari M, Jones EG (1990) A microcolumnar structure of monkey cerebral cortex revealed by immunocytochemical studies of double bouquet cell axons. Neuroscience 37:655-673.

del Rio MR, DeFelipe J (1995) A light and electron microscopic study of calbindin D-28k immunoreactive double bouquet cells in the human temporal cortex. Brain Res 690:133-140.

Destexhe A, Sejnowski T (2001) Thalamocortical Assembly. Oxford: Oxford University Press.

Deuchars J, West DC, Thomson AM (1994) Relationships between morphology and physiology of pyramid-pyramid single axon connections in rat neocortex in vitro. J Physiol 478 Pt 3:423-435.

Dossi RC, Nunez A, Steriade M (1992) Electrophysiology of a slow (0.5-4 Hz) intrinsic oscillation of cat thalamocortical neurones in vivo. J Physiol 447:215-234.

Espinosa F, Marks G, Heintz N, Joho RH (2004) Increased motor drive and sleep loss in mice lacking Kv3-type potassium channels. Genes Brain Behav 3:90-100.

Fairen A, Valverde F (1980) A specialized type of neuron in the visual cortex of cat: a Golgi and electron microscope study of chandelier cells. J Comp Neurol 194:761-779.

Fairen A, De Felipe J, Regidor J (1984) Nonpyramidal neurons. General account. In: Cerebral Cortex, Cellular components of the cerebral cortex (Peters A, Jones EG, eds), pp 201-253. New York: Plenum Press.

Feldman ML, Peters A (1978) The forms of non-pyramidal neurons in the visual cortex of the rat. J Comp Neurol 179:761-793.

Fisken RA, Garey LJ, Powell TP (1975) The intrinsic, association and commissural connections of area 17 on the visual cortex. Philos Trans R Soc Lond B Biol Sci 272:487-536.

Fleidervish IA, Gutnick MJ (1996) Kinetics of slow inactivation of persistent sodium current in layer V neurons of mouse neocortical slices. J Neurophysiol 76:2125-2130.

Fleidervish IA, Friedman A, Gutnick MJ (1996) Slow inactivation of Na+ current and slow cumulative spike adaptation in mouse and guinea-pig neocortical neurones in slices. J Physiol 493 (Pt 1):83-97.

Freeman WJ (1991) The physiology of perception. Sci Am 264:78-85.

Fuentealba P, Steriade M (2005) The reticular nucleus revisited: intrinsic and network properties of a thalamic pacemaker. Prog Neurobiol 75:125-141.

Fuentealba P, Crochet S, Steriade M (2004a) The cortically evoked secondary depolarization affects the integrative properties of thalamic reticular neurons. Eur J Neurosci 20:2691-2696.

Fuentealba P, Timofeev I, Steriade M (2004b) Prolonged hyperpolarizing potentials precede spindle oscillations in the thalamic reticular nucleus. Proc Natl Acad Sci U S A 101:9816-9821.

Fuentealba P, Timofeev I, Bazhenov M, Sejnowski TJ, Steriade M (2005) Membrane bistability in thalamic reticular neurons during spindle oscillations. J Neurophysiol 93:294-304.

Fuentealba P, Crochet S, Timofeev I, Bazhenov M, Sejnowski TJ, Steriade M (2004c) Experimental evidence and modeling studies support a synchronizing role for

electrical coupling in the cat thalamic reticular neurons in vivo. Eur J Neurosci 20:111-119.
Fujita I, Fujita T (1996) Intrinsic Connections in the macaque inferior temporal cortex. J Comp Neurol 368:467-486.
Gabbott PL, Martin KA, Whitteridge D (1987) Connections between pyramidal neurons in layer 5 of cat visual cortex (area 17). J Comp Neurol 259:364-381.
Gais S, Plihal W, Wagner U, Born J (2000) Early sleep triggers memory for early visual discrimination skills. Nat Neurosci 3:1335-1339.
Galarreta M, Hestrin S (1999) A network of fast-spiking cells in the neocortex connected by electrical synapses. Nature 402:72-75.
Galarreta M, Hestrin S (2001) Electrical synapses between GABA-releasing interneurons. Nat Rev Neurosci 2:425-433.
Garey LJ, Powell TP (1971) An experimental study of the termination of the lateral geniculo-cortical pathway in the cat and monkey. Proc R Soc Lond B Biol Sci 179:41-63.
Gentet LJ, Ulrich D (2003) Strong, reliable and precise synaptic connections between thalamic relay cells and neurones of the nucleus reticularis in juvenile rats. J Physiol 546:801-811.
Gibson JR, Beierlein M, Connors BW (1999) Two networks of electrically coupled inhibitory neurons in neocortex. Nature 402:75-79.
Gilbert CD (1983) Microcircuitry of the visual cortex. Annu Rev Neurosci 6:217-247.
Gilbert CD (1993) Circuitry, architecture, and functional dynamics of visual cortex. Cereb Cortex 3:373-386.
Gilbert CD, Wiesel TN (1979) Morphology and intracortical projections of functionally characterised neurones in the cat visual cortex. Nature 280:120-125.
Gilbert CD, Wiesel TN (1983) Clustered intrinsic connections in cat visual cortex. J Neurosci 3:1116-1133.
Gilbert CD, Wiesel TN (1989) Columnar specificity of intrinsic horizontal and corticocortical connections in cat visual cortex. J Neurosci 9:2432-2442.
Golshani P, Liu XB, Jones EG (2001) Differences in quantal amplitude reflect GluR4-subunit number at corticothalamic synapses on two populations of thalamic neurons. Proc Natl Acad Sci U S A 98:4172-4177.
Gray CM, McCormick DA (1996) Chattering cells: superficial pyramidal neurons contributing to the generation of synchronous oscillations in the visual cortex. Science 274:109-113.
Gray CM, Konig P, Engel AK, Singer W (1989) Oscillatory responses in cat visual cortex exhibit inter-columnar synchronization which reflects global stimulus properties. Nature 338:334-337.
Grenier F, Timofeev I, Steriade M (2001) Focal synchronization of ripples (80-200 Hz) in neocortex and their neuronal correlates. J Neurophysiol 86:1884-1898.
Gupta A, Wang Y, Markram H (2000) Organizing principles for a diversity of GABAergic interneurons and synapses in the neocortex. Science 287:273-278.
Hersch SM, White EL (1981) Quantification of synapses formed with apical dendrites of Golgi-impregnated pyramidal cells: variability in thalamocortical inputs, but consistency in the ratios of asymmetrical to symmetrical synapses. Neuroscience 6:1043-1051.

Hersch SM, White EL (1982) A quantitative study of the thalamocortical and other synapses in layer IV of pyramidal cells projecting from mouse SmI cortex to the caudate-putamen nucleus. J Comp Neurol 211:217-225.

Hestrin S, Armstrong WE (1996) Morphology and physiology of cortical neurons in layer I. J Neurosci 16:5290-5300.

Hill S, Tononi G (2005) Modeling sleep and wakefulness in the thalamocortical system. J Neurophysiol 93:1671-1698.

Hirsch JA, Alonso JM, Reid RC, Martinez LM (1998) Synaptic integration in striate cortical simple cells. J Neurosci 18:9517-9528.

Hirsch JC, Fourment A, Marc ME (1983) Sleep-related variations of membrane potential in the lateral geniculate body relay neurons of the cat. Brain Res 259:308-312.

Hollander H, Vanegas H (1981) Identification of pericellular baskets in the cat striate cortex: light and electron microscopic observations after uptake of horseradish peroxidase. J Neurocytol 10:577-587.

Huber R, Ghilardi MF, Massimini M, Tononi G (2004) Local sleep and learning. Nature 430:78-81.

Huguenard JR (1996) Low-threshold calcium currents in central nervous system neurons. Annu Rev Physiol 58:329-348.

Hustler J, Galuske AW (2003) Hemispheric asymetries in cerebral cortical networks. Trends Neurosci 26:429-435.

Ichikawa M, Arissian K, Asanuma H (1985) Distribution of corticocortical and thalamocortical synapses on identified motor cortical neurons in the cat: Golgi, electron microscopic and degeneration study. Brain Res 345:87-101.

Jones EG (1975) Varieties and distribution of non-pyramidal cells in the somatic sensory cortex of the squirrel monkey. J Comp Neurol 160:205-267.

Jones EG (1985) The thalamus. New York: Plenum.

Jones EG, Powell TP (1970) An electron microscopic study of the laminar pattern and mode of termination of afferent fibre pathways in the somatic sensory cortex of the cat. Philos Trans R Soc Lond B Biol Sci 257:45-62.

Keller A (1993) Intrinsic synaptic organization of the motor cortex. Cereb Cortex 3:430-441.

Kisvarday ZF, Martin KA, Freund TF, Magloczky Z, Whitteridge D, Somogyi P (1986) Synaptic targets of HRP-filled layer III pyramidal cells in the cat striate cortex. Exp Brain Res 64:541-552.

Krimer LS, Goldman-Rakic PS (2001) Prefrontal microcircuits: membrane properties and excitatory input of local, medium, and wide arbor interneurons. J Neurosci 21:3788-3796.

Kritzer MF, Goldman-Rakic PS (1995) Intrinsic circuit organization of the major layers and sublayers of the dorsolateral prefrontal cortex in the rhesus monkey. J Comp Neurol 359:131-143.

Kuljis RO, Rakic P (1989) Distribution of neuropeptide Y-containing perikarya and axons in various neocortical areas in the macaque monkey. J Comp Neurol 280:383-392.

Landisman CE, Long MA, Beierlein M, Deans MR, Paul DL, Connors BW (2002) Electrical synapses in the thalamic reticular nucleus. J Neurosci 22:1002-1009.

Leresche N, Lightowler S, Soltesz I, Jassik-Gerschenfeld D, Crunelli V (1991) Low-frequency oscillatory activities intrinsic to rat and cat thalamocortical cells. J Physiol 441:155-174.

LeVay S (1973) Synaptic patterns in the visual cortex of the cat and monkey. Electron microscopy of Golgi preparations. J Comp Neurol 150:53-85.
Lisman JE (1997) Bursts as a unit of neural information: making unreliable synapses reliable. Trends Neurosci 20:38-43.
Loomis AL, Harvey EN, Hobart GA (1937) Cerebral states during sleep, as studied by human brain potentials. J Exp Psychol 21:127-144.
Lorente de No R (1922) La corteza cerebral del raton. trab lab Invest Biol Madrid 20:41-78.
Lowenstein PR, Somogyi P (1991) Synaptic organization of cortico-cortical connections from the primary visual cortex to the posteromedial lateral suprasylvian visual area in the cat. J Comp Neurol 310:253-266.
Lund JS (1973) Organization of neurons in the visual cortex, area 17, of the monkey (Macaca mulatta). J Comp Neurol 147:455-496.
Lund JS (1987) Local circuit neurons of macaque monkey striate cortex: I. Neurons of laminae 4C and 5A. J Comp Neurol 257:60-92.
Lund JS (1988) Anatomical organization of macaque monkey striate visual cortex. Annu Rev Neurosci 11:253-288.
Lund JS, Lund RD (1970) The termination of callosal fibers in the paravisual cortex of the rat. Brain Res 17:25-45.
Lund JS, Yoshioka T, Levitt JB (1993) Comparison of intrinsic connectivity in different areas of macaque monkey cerebral cortex. Cereb Cortex 3:148-162.
Luthi A, Bal T, McCormick DA (1998) Periodicity of thalamic spindle waves is abolished by ZD7288,a blocker of Ih. J Neurophysiol 79:3284-3289.
Magee JC, Cook EP (2000) Somatic EPSP amplitude is independent of synapse location in hippocampal pyramidal neurons. Nat Neurosci 3:895-903.
Maquet P (2001) The role of sleep in learning and memory. Science 294:1048-1052.
Marin-Padilla M (1969) Origin of the pericellular baskets of the pyramidal cells of the human motor cortex: a Golgi study. Brain Res 14:633-646.
Marin-Padilla M (1974) Three-dimensional reconstruction of the pericellular nests (baskets) of the motor (area 4) and visual (area 17) areas of the human cerebral cortex. A Golgi study. Z Anat Entwicklungsgesch 144:123-135.
Marin-Padilla M (1987) The chandelier cell of the human visual cortex: a Golgi study. J Comp Neurol 256:61-70.
Marin-Padilla M, Stibitz GR (1974) Three-dimensional reconstruction of the basket cell of the human motor cortex. Brain Res 70:511-514.
Markram H, Tsodyks M (1996) Redistribution of synaptic efficacy between neocortical pyramidal neurons. Nature 382:807-810.
Markram H, Lubke J, Frotscher M, Roth A, Sakmann B (1997) Physiology and anatomy of synaptic connections between thick tufted pyramidal neurones in the developing rat neocortex. J Physiol 500 (Pt 2):409-440.
Markram H, Toledo-Rodriguez M, Wang Y, Gupta A, Silberberg G, Wu C (2004) Interneurons of the neocortical inhibitory system. Nat Rev Neurosci 5:793-807.
Martin KA, Whitteridge D (1984) Form, function and intracortical projections of spiny neurones in the striate visual cortex of the cat. J Physiol 353:463-504.
Massimini M, Amzica F (2001) Extracellular calcium fluctuations and intracellular potentials in the cortex during the slow sleep oscillation. J Neurophysiol 85:1346-1350.

Mates SL, Lund JS (1983) Neuronal composition and development in lamina 4C of monkey striate cortex. J Comp Neurol 221:60-90.

McCormick DA (1992) Neurotransmitter actions in the thalamus and cerebral cortex and their role in neuromodulation of thalamocortical activity. Prog Neurobiol 39:337-388.

McCormick DA, Pape HC (1990) Properties of a hyperpolarization-activated cation current and its role in rhythmic oscillation in thalamic relay neurones. J Physiol 431:291-318.

McCormick DA, Connors BW, Lighthall JW, Prince DA (1985) Comparative electrophysiology of pyramidal and sparsely spiny stellate neurons of the neocortex. J Neurophysiol 54:782-806.

McGuire BA, Hornung JP, Gilbert CD, Wiesel TN (1984) Patterns of synaptic input to layer 4 of cat striate cortex. J Neurosci 4:3021-3033.

McGuire BA, Gilbert CD, Rivlin PK, Wiesel TN (1991) Targets of horizontal connections in macaque primary visual cortex. J Comp Neurol 305:370-392.

Metherate R, Ashe JH (1993) Ionic flux contributions to neocortical slow waves and nucleus basalis-mediated activation: whole-cell recordings in vivo. J Neurosci 13:5312-5323.

Mountcastle VB (1997) The columnar organization of the neocortex. Brain 120 (Pt 4):701-722.

Mountcastle VB (1998) Chapter 3: Cells and local networks of the neocortex. In: Perceptual Neuroscience, The cerebral cortex, p 486. Cambridge, Massachusetts: Harvard University Press.

Mukhametov LM, Rizzolatti G, Tradardi V (1970) Spontaneous activity of neurones of nucleus reticularis thalami in freely moving cats. J Physiol 210:651-667.

Mukovski M, Chauvette S, Boucetta S, Timofeev I, Volgushev M (Submitted 2005)) Detection of active and silent states in neocortical neurons from the field potential signal. J Neurosci.

Murthy VN, Fetz EE (1992) Coherent 25- to 35-Hz oscillations in the sensorimotor cortex of awake behaving monkeys. Proc Natl Acad Sci U S A 89:5670-5674.

Niedermeyer E (1993a) Chapter 9. The normal EEG of the waking adult. In: Electroencephalography. Basic principles, clinical applications, and related fields, third Edition (Wilkins W, ed), p 1164. Baltimore.

Niedermeyer E (1993b) Chapter 10. Sleep and EEG. In: Electroencephalography. Basic principles, clinical applications, and related fields, third Edition (Wilkins W, ed), p 1164. Baltimore.

Nishimura Y, Asahi M, Saitoh K, Kitagawa H, Kumazawa Y, Itoh K, Lin M, Akamine T, Shibuya H, Asahara T, Yamamoto T (2001) Ionic mechanisms underlying burst firing of layer III sensorimotor cortical neurons of the cat: an in vitro slice study. J Neurophysiol 86:771-781.

Nunez A, Amzica F, Steriade M (1993) Electrophysiology of cat association cortical cells in vivo: intrinsic properties and synaptic responses. J Neurophysiol 70:418-430.

Ojima H, Honda CN, Jones EG (1991) Patterns of axon collateralization of identified supragranular pyramidal neurons in the cat auditory cortex. Cereb Cortex 1:80-94.

Pape HC (1996) Queer current and pacemaker: the hyperpolarization-activated cation current in neurons. Annu Rev Physiol 58:299-327.

Parnavelas JG, Lieberman AR, Webster KE (1977) Organization of neurons in the visual cortex, area 17, of the rat. J Anat 124:305-322.
Peters A (1987) Number of neurons and synapses in primary visual cortex. In: Cerebral cortex, Further aspects of cortical function, including hippocampus (Jones EG, Peters A, eds), pp 267-294. New York: Plenum Press.
Peters A, Feldman ML (1976) The projection of the lateral geniculate nucleus to area 17 of the rat cerebral cortex. I. General description. J Neurocytol 5:63-84.
Peters A, Regidor J (1981) A reassessment of the forms of nonpyramidal neurons in area 17 of cat visual cortex. J Comp Neurol 203:685-716.
Peters A, Kimerer LM (1981) Bipolar neurons in rat visual cortex: a combined Golgi-electron microscope study. J Neurocytol 10:921-946.
Peters A, Harriman KM (1988) Enigmatic bipolar cell of rat visual cortex. J Comp Neurol 267:409-432.
Peters A, Palay SL, Webster Hd (1991) The fine structure of the nervous system. Neurons and their supporting cells. New York: Oxford University Press.
Pfurtscheller G, Neuper C (1992) Simultaneous EEG 10 Hz desynchronization and 40 Hz synchronization during finger movements. Neuroreport 3:1057-1060.
Porter LL, White EL (1986) Synaptic connections of callosal projection neurons in the vibrissal region of mouse primary motor cortex: an electron microscopic/horseradish peroxidase study. J Comp Neurol 248:573-587.
Porter LL, Sakamoto K (1988) Organization and synaptic relationships of the projection from the primary sensory to the primary motor cortex in the cat. J Comp Neurol 271:387-396.
Rockland KS, Lund JS (1982) Widespread periodic intrinsic connections in the tree shrew visual cortex. Science 215:1532-1534.
Rosanova M, Timofeev I (2005) Neuronal mechanisms mediating the variability of somatosensory evoked potentials during sleep oscillations in cats. J Physiol 562:569-582.
Rougeul-Buser A, Bouyer JJ, Buser P (1975) From attentiveness to sleep. A topographical analysis of localized "synchronized" activities on the cortex of normal cat and monkey. Acta Neurobiol Exp (Wars) 35:805-819.
Saint Marie RL, Peters A (1985) The morphology and synaptic connections of spiny stellate neurons in monkey visual cortex (area 17): a Golgi-electron microscopic study. J Comp Neurol 233:213-235.
Sanchez-Vives MV, McCormick DA (2000) Cellular and network mechanisms of rhythmic recurrent activity in neocortex. Nat Neurosci 3:1027-1034.
Schmitz D, Schuchmann S, Fisahn A, Draguhn A, Buhl EH, Petrasch-Parwez E, Dermietzel R, Heinemann U, Traub RD (2001) Axo-axonal coupling. a novel mechanism for ultrafast neuronal communication. Neuron 31:831-840.
Schwark HD, Jones EG (1989) The distribution of intrinsic cortical axons in area 3b of cat primary somatosensory cortex. Exp Brain Res 78:501-513.
Schwindt PC, Spain WJ, Crill WE (1989) Long-lasting reduction of excitability by a sodium-dependent potassium current in cat neocortical neurons. J Neurophysiol 61:233-244.
Schwindt PC, Spain WJ, Crill WE (1992) Calcium-dependent potassium currents in neurons from cat sensorimotor cortex. J Neurophysiol 67:216-226.

Shaw PJ, Cirelli C, Greenspan RJ, Tononi G (2000) Correlates of sleep and waking in Drosophila melanogaster. Science 287:1834-1837.
Sheer DE (1989) Focused arousal and the cognitive 40-Hz event-related potentials: differential diagnosis of Alzheimer's disease. Prog Clin Biol Res 317:79-94.
Sholl DA (1955) The surface area of cortical neurons. J Anat 89:33-46.
Sloper JJ (1973) An electron microscope study of the termination of afferent connections to the primate motor cortex. J Neurocytol 2:361-368.
Sloper JJ, Powell TP (1979) An experimental electron microscopic study of afferent connections to the primate motor and somatic sensory cortices. Philos Trans R Soc Lond B Biol Sci 285:199-226.
Soderling TR, Derkach VA (2000) Postsynaptic protein phosphorylation and LTP. Trends Neurosci 23:75-80.
Soltesz I, Lightowler S, Leresche N, Jassik-Gerschenfeld D, Pollard CE, Crunelli V (1991) Two inward currents and the transformation of low-frequency oscillations of rat and cat thalamocortical cells. J Physiol 441:175-197.
Somogyi P (1977) A specific 'axo-axonal' interneuron in the visual cortex of the rat. Brain Res 136:345-350.
Somogyi P (1978) The study of Golgi stained cells and of experimental degeneration under the electron microscope: a direct method for the identification in the visual cortex of three successive links in a neuron chain. Neuroscience 3:167-180.
Somogyi P, Cowey A (1981) Combined Golgi and electron microscopic study on the synapses formed by double bouquet cells in the visual cortex of the cat and monkey. J Comp Neurol 195:547-566.
Somogyi P, Freund TF, Cowey A (1982) The axo-axonic interneuron in the cerebral cortex of the rat, cat and monkey. Neuroscience 7:2577-2607.
Somogyi P, Kisvarday ZF, Martin KA, Whitteridge D (1983) Synaptic connections of morphologically identified and physiologically characterized large basket cells in the striate cortex of cat. Neuroscience 10:261-294.
Somogyi P, Tamas G, Lujan R, Buhl EH (1998) Salient features of synaptic organisation in the cerebral cortex. Brain Res Brain Res Rev 26:113-135.
Spatz WB, Tigges J, Tigges M (1970) Subcortical projections, cortical associations, and some intrinsic interlaminar connections of the striate cortex in the squirrel monkey (Saimiri). J Comp Neurol 140:155-174.
Squire B, McConnell, Roberts, Spitzer, Zigmond (2003) Chapter 3: Cellular components of nervous tissue. In: Fundamental Neuroscience, Second Edition. San Diego, California: Academic Press.
Steriade M (2000) Corticothalamic resonance, states of vigilance and mentation. Neuroscience 101:243-276.
Steriade M (2001a) The intact and sliced brain. In: The intact and sliced brain, The MIT Press Edition (press TM, ed), p 366. Cambridge, Massachusetts.
Steriade M (2001b) Impact of network activities on neuronal properties in corticothalamic systems. J Neurophysiol 86:1-39.
Steriade M (2004a) Neocortical cell classes are flexible entities. Nat Rev Neurosci 5:121-134.
Steriade M (2004b) Acetylcholine systems and rhythmic activities during the waking--sleep cycle. Prog Brain Res 145:179-196.

Steriade M, Wyzinski P (1972) Cortically elicited activities in thalamic reticularis neurons. Brain Res 42:514-520.
Steriade M, McCarley RW (1990) Brainstem Control of Wakefulness and Sleep. New York: Plenum.
Steriade M, Timofeev I (2003) Neuronal plasticity in thalamocortical networks during sleep and waking oscillations. Neuron 37:563-576.
Steriade M, Domich L, Oakson G (1986) Reticularis thalami neurons revisited: activity changes during shifts in states of vigilance. J Neurosci 6:68-81.
Steriade M, Nunez A, Amzica F (1993a) A novel slow (< 1 Hz) oscillation of neocortical neurons in vivo: depolarizing and hyperpolarizing components. J Neurosci 13:3252-3265.
Steriade M, Nunez A, Amzica F (1993b) Intracellular analysis of relations between the slow (< 1 Hz) neocortical oscillation and other sleep rhythms of the electroencephalogram. J Neurosci 13:3266-3283.
Steriade M, Amzica F, Contreras D (1996a) Synchronization of fast (30-40 Hz) spontaneous cortical rhythms during brain activation. J Neurosci 16:392-417.
Steriade M, Jones EG, McCormick DA (1997) Thalamus: organization and function. Kidlington, Oxford: Elsevier Science Ltd.
Steriade M, Timofeev I, Grenier F (2000) Input resistance of cortical neurons during natural states of vigilance in behaving cats. In: Soc. Neurosci. Abstr. New Orleans, La.
Steriade M, Timofeev I, Grenier F (2001) Natural waking and sleep states: a view from inside neocortical neurons. J Neurophysiol 85:1969-1985.
Steriade M, Deschenes M, Domich L, Mulle C (1985) Abolition of spindle oscillations in thalamic neurons disconnected from nucleus reticularis thalami. J Neurophysiol 54:1473-1497.
Steriade M, Domich L, Oakson G, Deschenes M (1987) The deafferented reticular thalamic nucleus generates spindle rhythmicity. J Neurophysiol 57:260-273.
Steriade M, Contreras D, Amzica F, Timofeev I (1996b) Synchronization of fast (30-40 Hz) spontaneous oscillations in intrathalamic and thalamocortical networks. J Neurosci 16:2788-2808.
Steriade M, Timofeev I, Durmuller N, Grenier F (1998) Dynamic properties of corticothalamic neurons and local cortical interneurons generating fast rhythmic (30-40 Hz) spike bursts. J Neurophysiol 79:483-490.
Stickgold R, James L, Hobson JA (2000a) Visual discrimination learning requires sleep after training. Nat Neurosci 3:1237-1238.
Stickgold R, Whidbee D, Schirmer B, Patel V, Hobson JA (2000b) Visual discrimination task improvement: A multi-step process occurring during sleep. J Cogn Neurosci 12:246-254.
Stratford KJ, Tarczy-Hornoch K, Martin KA, Bannister NJ, Jack JJ (1996) Excitatory synaptic inputs to spiny stellate cells in cat visual cortex. Nature 382:258-261.
Szentagothai J (1975) The 'module-concept' in cerebral cortex architecture. Brain Res 95:475-496.
Szentagothai J (1978) The Ferrier Lecture, 1977. The neuron network of the cerebral cortex: a functional interpretation. Proc R Soc Lond B Biol Sci 201:219-248.
Szentagothai J, Arbib MA (1974) Conceptual models of neural organization. Neurosci Res Program Bull 12:305-510.

Tamas G, Somogyi P, Buhl EH (1998) Differentially interconnected networks of GABAergic interneurons in the visual cortex of the cat. J Neurosci 18:4255-4270.
Thimm J, Mechler A, Lin H, Rhee S, Lal R (2005) Calcium-dependent open/closed conformations and interfacial energy maps of reconstituted hemichannels. J Biol Chem 280:10646-10654.
Thomson AM, Deuchars J (1997) Synaptic interactions in neocortical local circuits: dual intracellular recordings in vitro. Cereb Cortex 7:510-522.
Thomson AM, Bannister AP (2003) Interlaminar connections in the neocortex. Cereb Cortex 13:5-14.
Thomson AM, West DC, Deuchars J (1995) Properties of single axon excitatory postsynaptic potentials elicited in spiny interneurons by action potentials in pyramidal neurons in slices of rat neocortex. Neuroscience 69:727-738.
Thomson AM, West DC, Hahn J, Deuchars J (1996) Single axon IPSPs elicited in pyramidal cells by three classes of interneurones in slices of rat neocortex. J Physiol 496 (Pt 1):81-102.
Thomson AM, West DC, Wang Y, Bannister AP (2002) Synaptic connections and small circuits involving excitatory and inhibitory neurons in layers 2-5 of adult rat and cat neocortex: triple intracellular recordings and biocytin labelling in vitro. Cereb Cortex 12:936-953.
Timofeev I, Steriade M (1996) Low-frequency rhythms in the thalamus of intact-cortex and decorticated cats. J Neurophysiol 76:4152-4168.
Timofeev I, Steriade M (1997) Fast (mainly 30-100 Hz) oscillations in the cat cerebellothalamic pathway and their synchronization with cortical potentials. J Physiol 504 (Pt 1):153-168.
Timofeev I, Bazhenov M (2005) Chapter I: Mechanisms and biological role of thalamocortical oscillations. In: Trends in Chronobiology Research (Columbus F, ed), pp pp. 1-47: Nova Science Publishers, Inc.
Timofeev I, Contreras D, Steriade M (1996) Synaptic responsiveness of cortical and thalamic neurones during various phases of slow sleep oscillation in cat. J Physiol 494 (Pt 1):265-278.
Timofeev I, Grenier F, Steriade M (2000a) Impact of intrinsic properties and synaptic factors on the activity of neocortical networks in vivo. J Physiol Paris 94:343-355.
Timofeev I, Grenier F, Steriade M (2001a) Disfacilitation and active inhibition in the neocortex during the natural sleep-wake cycle: an intracellular study. Proc Natl Acad Sci U S A 98:1924-1929.
Timofeev I, Bazhenov M, Sejnowski TJ, Steriade M (2001b) Contribution of intrinsic and synaptic factors in the desynchronization of thalamic oscillatory activity. Thalamus & related Systems 1:53-69.
Timofeev I, Grenier F, Bazhenov M, Sejnowski TJ, Steriade M (2000b) Origin of slow cortical oscillations in deafferented cortical slabs. Cereb Cortex 10:1185-1199.
Traub RD, Buhl EH, Gloveli T, Whittington MA (2003) Fast rhythmic bursting can be induced in layer 2/3 cortical neurons by enhancing persistent Na+ conductance or by blocking BK channels. J Neurophysiol 89:909-921.
Tsodyks MV, Markram H (1997) The neural code between neocortical pyramidal neurons depends on neurotransmitter release probability. Proc Natl Acad Sci U S A 94:719-723.

Valverde F (1976) Aspects of cortical organization related to the geometry of neurons with intra-cortical axons. J Neurocytol 5:509-529.

Voigt T, LeVay S, Stamnes MA (1988) Morphological and immunocytochemical observations on the visual callosal projections in the cat. J Comp Neurol 272:450-460.

Vyazovskiy VV, Deboer T, Rudy B, Lau D, Borbely AA, Tobler I (2002) Sleep EEG in mice that are deficient in the potassium channel subunit K.v.3.2. Brain Res 947:204-211.

Wahle P (1993) Differential regulation of substance P and somatostatin in Martinotti cells of the developing cat visual cortex. J Comp Neurol 329:519-538.

Wang Y, Gupta A, Toledo-Rodriguez M, Wu CZ, Markram H (2002) Anatomical, physiological, molecular and circuit properties of nest basket cells in the developing somatosensory cortex. Cereb Cortex 12:395-410.

Wang Y, Toledo-Rodriguez M, Gupta A, Wu C, Silberberg G, Luo J, Markram H (2004) Anatomical, physiological and molecular properties of Martinotti cells in the somatosensory cortex of the juvenile rat. J Physiol 561:65-90.

Wang Z, McCormick DA (1993) Control of firing mode of corticotectal and corticopontine layer V burst-generating neurons by norepinephrine, acetylcholine, and 1S,3R-ACPD. J Neurosci 13:2199-2216.

Watts J, Thomson AM (2005) Excitatory and inhibitory connections show selectivity in the neocortex. J Physiol 562:89-97.

White EL (1989) Cortical circuits: Synaptic Organization of the cerebral cortex. Structure, Function and theory. Boston: Birkhäuser.

White EL, Hersch SM (1981) Thalamocortical synapses of pyramidal cells which project from SmI to MsI cortex in the mouse. J Comp Neurol 198:167-181.

White EL, Hersch SM (1982) A quantitative study of thalamocortical and other synapses involving the apical dendrites of corticothalamic projection cells in mouse SmI cortex. J Neurocytol 11:137-157.

Williams SR, Stuart GJ (2002) Dependence of EPSP efficacy on synapse location in neocortical pyramidal neurons. Science 295:1907-1910.

Williams SR, Stuart GJ (2003) Role of dendritic synapse location in the control of action potential output. Trends Neurosci 26:147-154.

Wilson CJ (1986) Postsynaptic potentials evoked in spiny neostriatal projection neurons by stimulation of ipsilateral and contralateral neocortex. Brain Res 367:201-213.

Wilson CJ, Chang HT, Kitai ST (1983) Disfacilitation and long-lasting inhibition of neostriatal neurons in the rat. Exp Brain Res 51:227-235.

Yoshioka T, Levitt JB, Lund JS (1994) Independence and merger of thalamocortical channels within macaque monkey primary visual cortex: anatomy of interlaminar projections. Vis Neurosci 11:467-489.

Yuste R, Tank DW (1996) Dendritic integration in mammalian neurons, a century after Cajal. Neuron 16:701-716.

Zhang ZW, Deschenes M (1997) Intracortical axonal projections of lamina VI cells of the primary somatosensory cortex in the rat: a single-cell labeling study. J Neurosci 17:6365-6379.